



UNITED NATIONS EDUCATIONAL, SCIENTIFIC AND CULTURAL ORGANIZATION
INTERNATIONAL ATOMIC ENERGY AGENCY
INTERNATIONAL CENTRE FOR THEORETICAL PHYSICS
I.C.T.P., P.O. BOX 586, 34100 TRIESTE, ITALY, CABLE: CENTRATOM TRIESTE



SMR.959 - 39

MINIWORKSHOP ON STRONG ELECTRON CORRELATIONS
"Disorder and Interaction in Quantum Systems
and Their Classical Analogs"

(1 - 19 July 1996)

"Colossal Magnetoresistance in Manganite Perovskites
and Related Compounds"

Arthur Ramirez
Bell Laboratories, Lucent Technologies
Murray Hill, NJ 07974
U.S.A.

These are preliminary lecture notes, intended only for distribution to participants.

Colossal Magnetoresistance
in
Manganite Perovskites
and
Related Compounds

Collaborators:

P. Schiffer (Notre Dame)

T. Palstra (→ Groningen)

G. Alers (BL)

P. Gammel (BL)

D. Bishop (BL)

C. Chen (BL)

G. Kwei (LLNL)

B. Toby (NIST)

M. Subramanian (DuPont)

S-W. Cheong (BL)

R. Cava (→ Princeton)

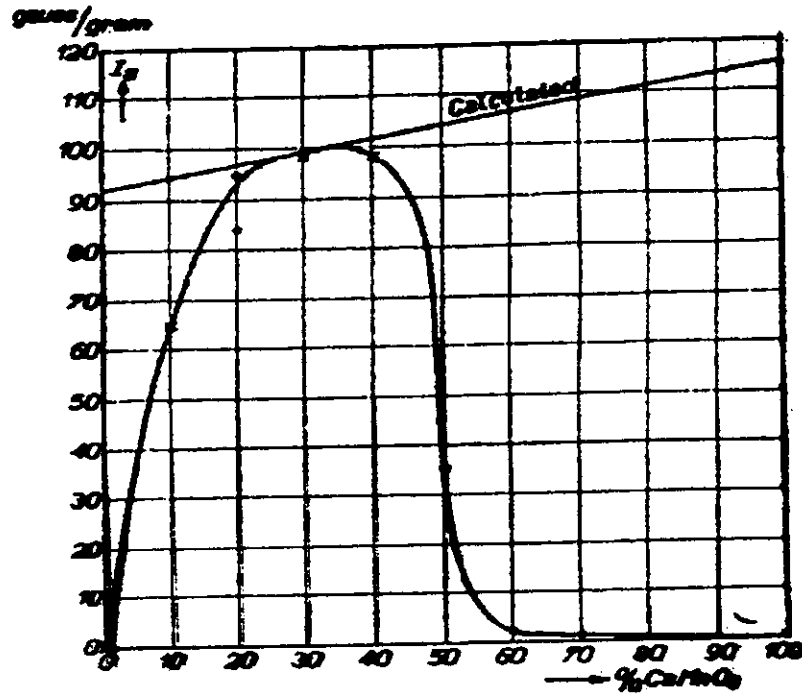
W. Bao (BNL)

P. McGinn (Notre Dame)

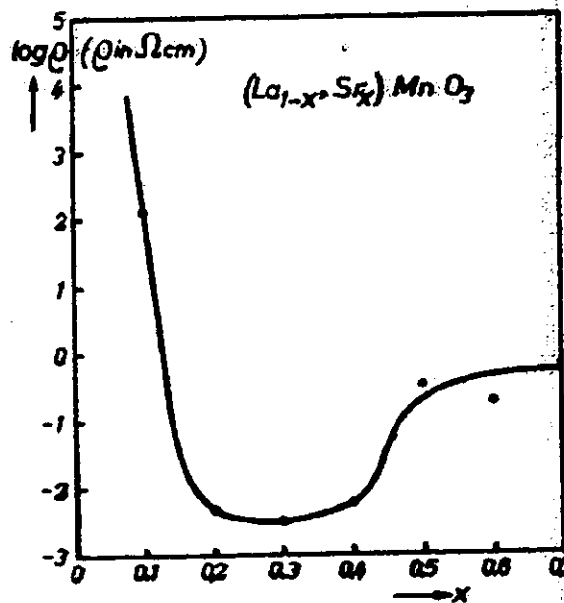
A. Sleight (Orgeon)

- CMR has potential for applications.
- Lattice effects extremely important.
- CMR found in other materials
besides Mn-O perovskites.

Magnetization of $\text{La}_{1-x}\text{Ca}_x\text{MnO}_3$ - (90 K)



Resistivity of $\text{La}_{1-x}\text{Sr}_x\text{MnO}_3$ (100 K)



How does magnetism and transport evolve as the ratio Mn^{4+}/Mn^{3+} increases?
 First look back at old neutron scattering work. Wollan and Koehler (1955)

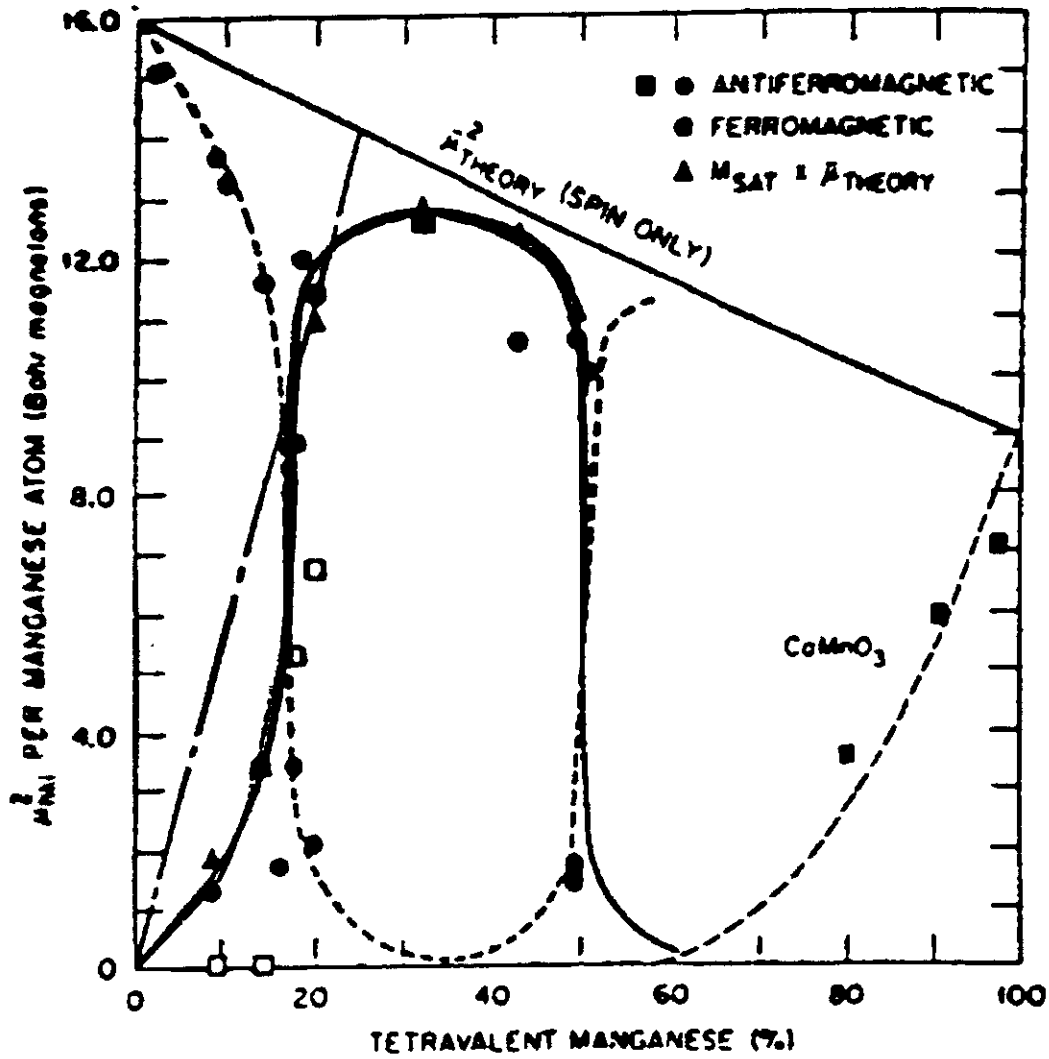
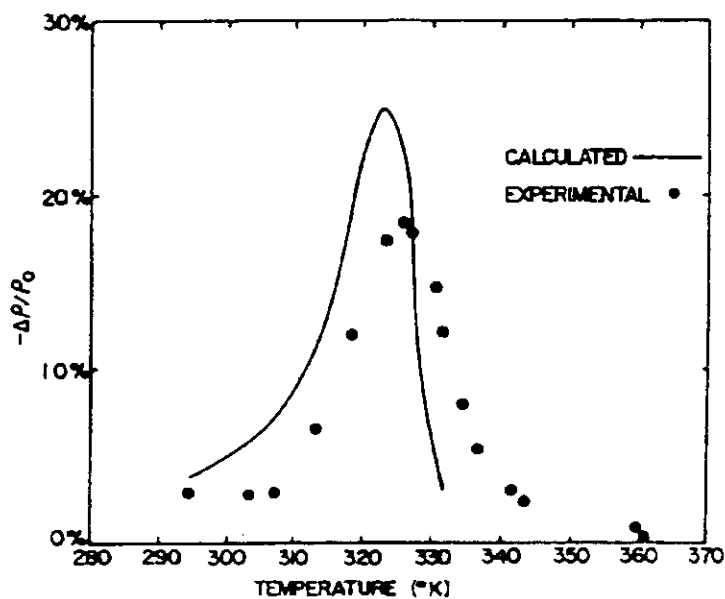
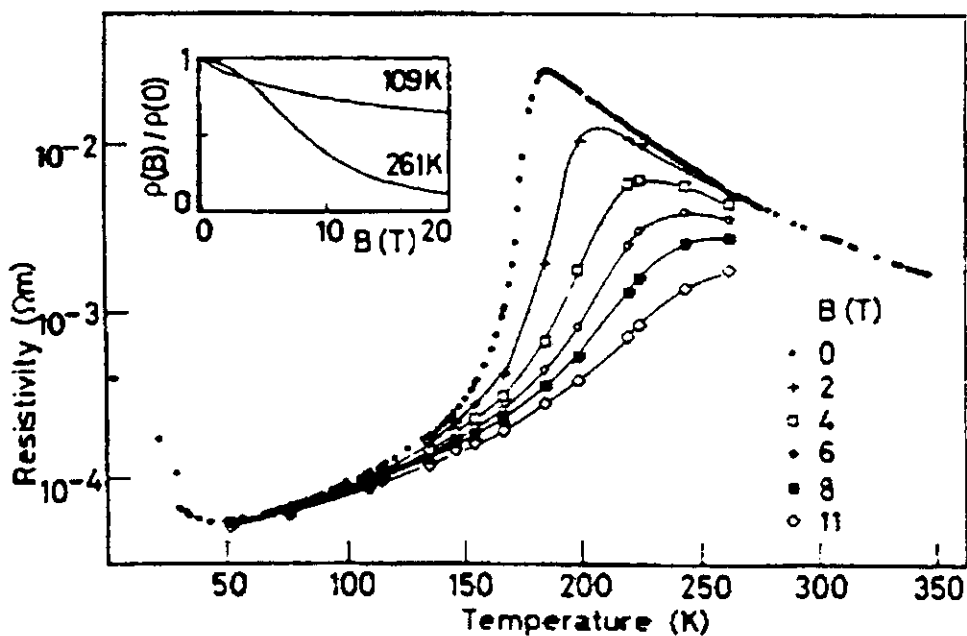


FIG. 19. Ferromagnetic and antiferromagnetic moments as a function of sample ion composition.

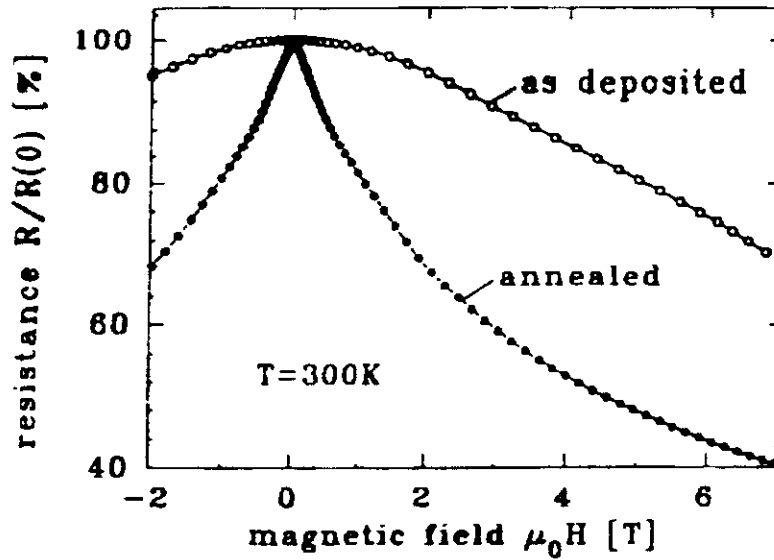
- More experimental work followed -
Searle & Wang (1969) - H-dependence - shown below is MR at 1 Tesla for $\text{La}_{0.69}\text{Pb}_{0.31}\text{MnO}_3$ -



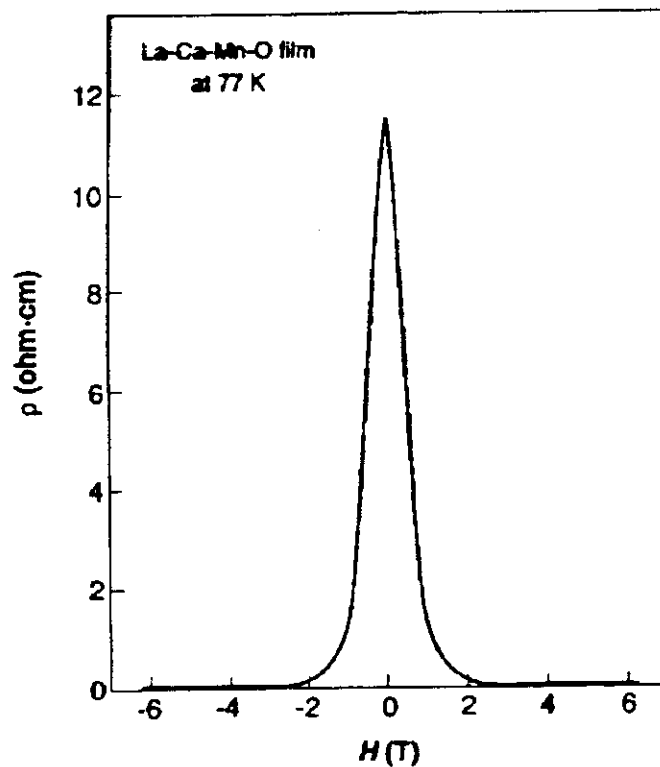
- Kusters et al. (1989) - High-field magnetoresistance and a suggestion of magnetic polaron transport in $\text{Nd}_{0.5}\text{Pb}_{0.5}\text{MnO}_3$.

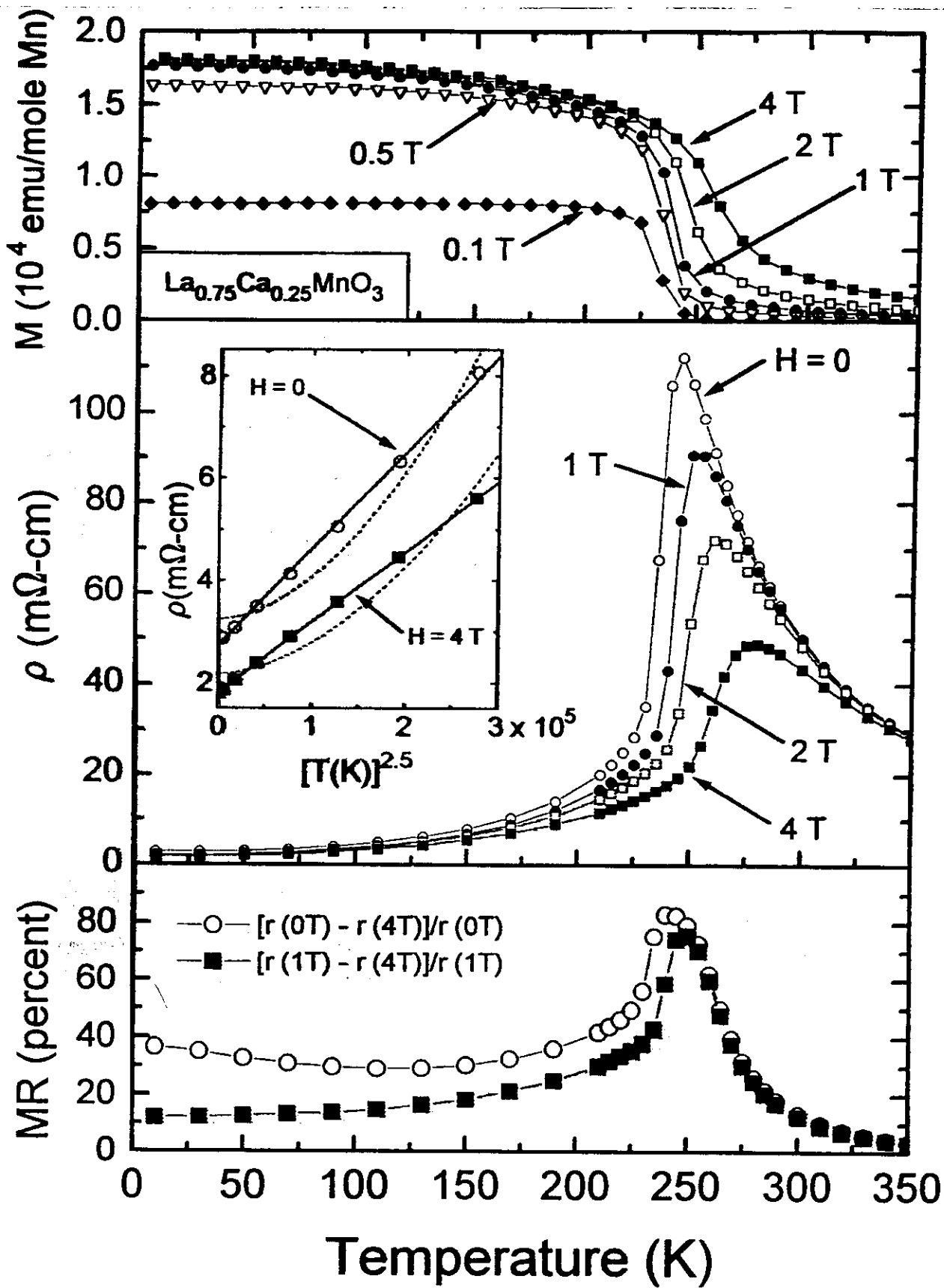


- von Helmolt et al. (1993) - Thin films (substrate clamping) reduce T_C and raise MR for epitaxial $\text{La}_{1-x}\text{Ba}_x\text{MnO}_3$ -



- Jin, McCormack (1994) - CMR effect (3 orders of magnitude change in R at 6 Tesla) can be enhanced by heat treating epitaxial films grown on LaAlO_3 substrates and lowering T_C .

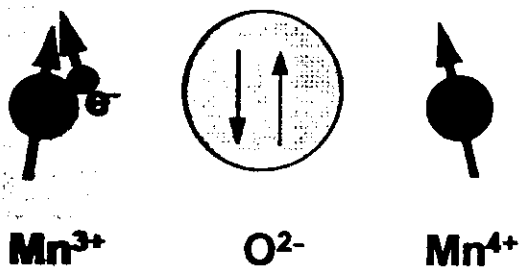




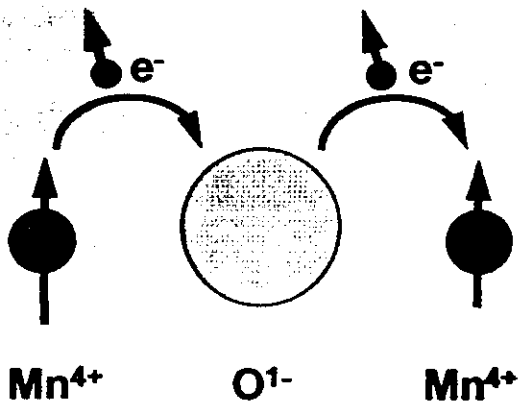
gmranal/75-25fg2

PRL
Schiffer et al., '95

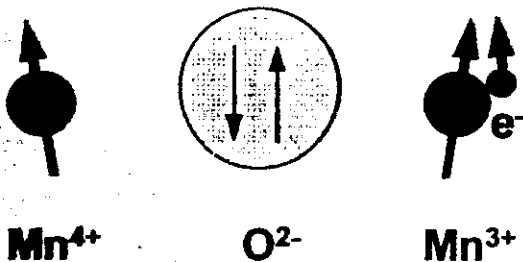
• Zener (1951) - "Double exchange"



Consider an inhomogeneously mixed valence (IMV) system of Hund's rule ions where hopping can proceed through an intervening anion.



Satisfy local constraints and hopping occurs through the simultaneous exchange to and from anion only when cation spins are parallel.

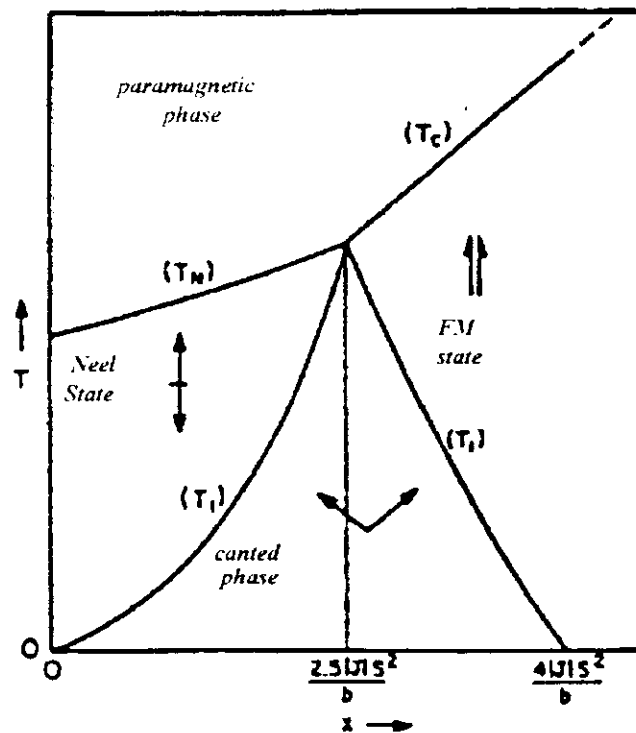


Final state degenerate with initial state.

- Anderson & Hasegawa ('55) -
 - Generalized Zener's idea to semiclassical spins (*interspin angle* θ)
 - Introduced higher-order processes. For large *intraatomic* exchange coupling, $J \gg b$ (transfer integral), energy of extra electron (hole) is:

$$E \cong -JS \pm b \cos(\theta/2).$$

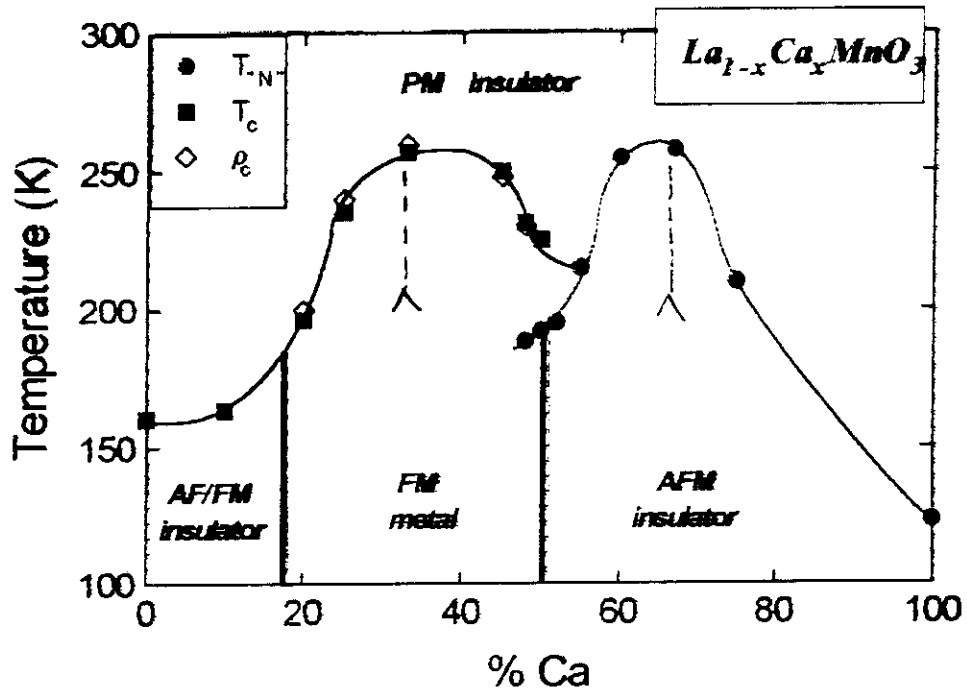
- DeGennes ('60) -
 - Any amount of doping in AF DE systems \rightarrow canted (FM) moment due to gain in kinetic energy of carrier when spins aligned.
 - Neglect of self trapping and trapping by Ca^{2+} sites not critical - still get localized canting.
 - Mean field theory \rightarrow phase diagram predicting distinct AF and FM transitions.



J here = *interatomic* exchange

Phase Diagram - $La_{1-x}Ca_xMnO_3$

Schiffer et al. PRL (1995)



Data Storage Industry

- ***Its big***
 - ▶ 23 B\$ in world wide revenue for disk drives in '94
 - ▶ 60 million drives sold in '94
 - ▶ about 600 million recording heads sold - each with a magnetic sensor
- ***Its getting bigger***
 - ▶ storage applications growing rapidly
 - ▶ fueled by image-hungry software



HEWLETT PACKARD LABORATORIES
THIN FILM DEPARTMENT
Jim Brug p950215



HEWLETT
PACKARD

CMR Requirements → for conventional recording

- **change in resistance**
 - ▶ $dR/R_0 > 90\%$
 - ↔ ▶ no need for huge effects - 90% is almost as good as $10^{10}\%$
- **field dependence**
 - ▶ really need it down to 100 Oe ⇒ 90% effect in 100 Oe
 - ▶ GMR will be good for 10% effects in 100 Oe
- **resistivity important as well**
 - ▶ signal / noise ratio is hurt by high resistance
 - ▶ no advantage to a high resistance
- **current carrying capacity important**
 - ▶ able to take high power density
 - ▶ 0.1 mwatt in a 1 um device
- *make it work at room T.*

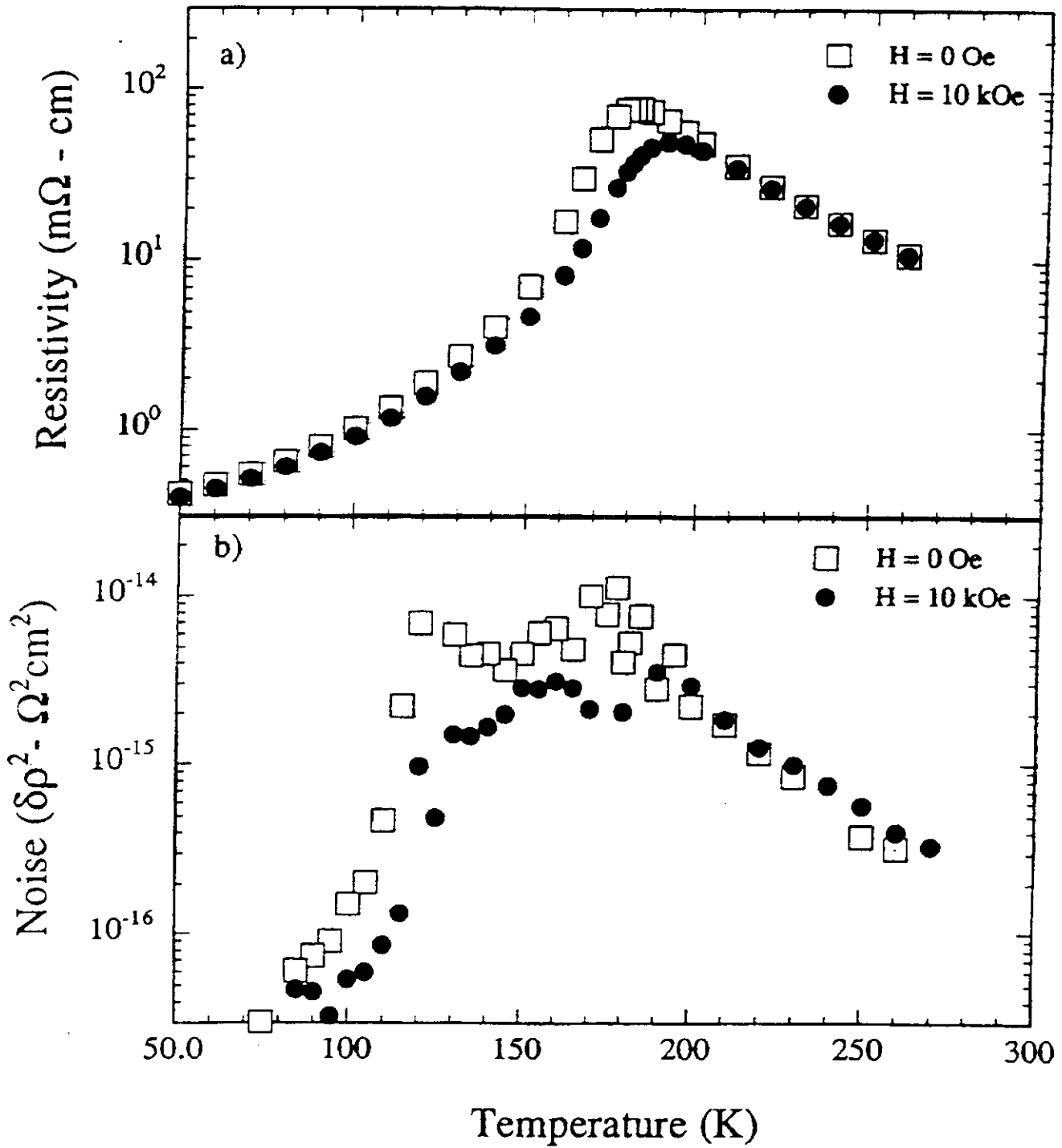


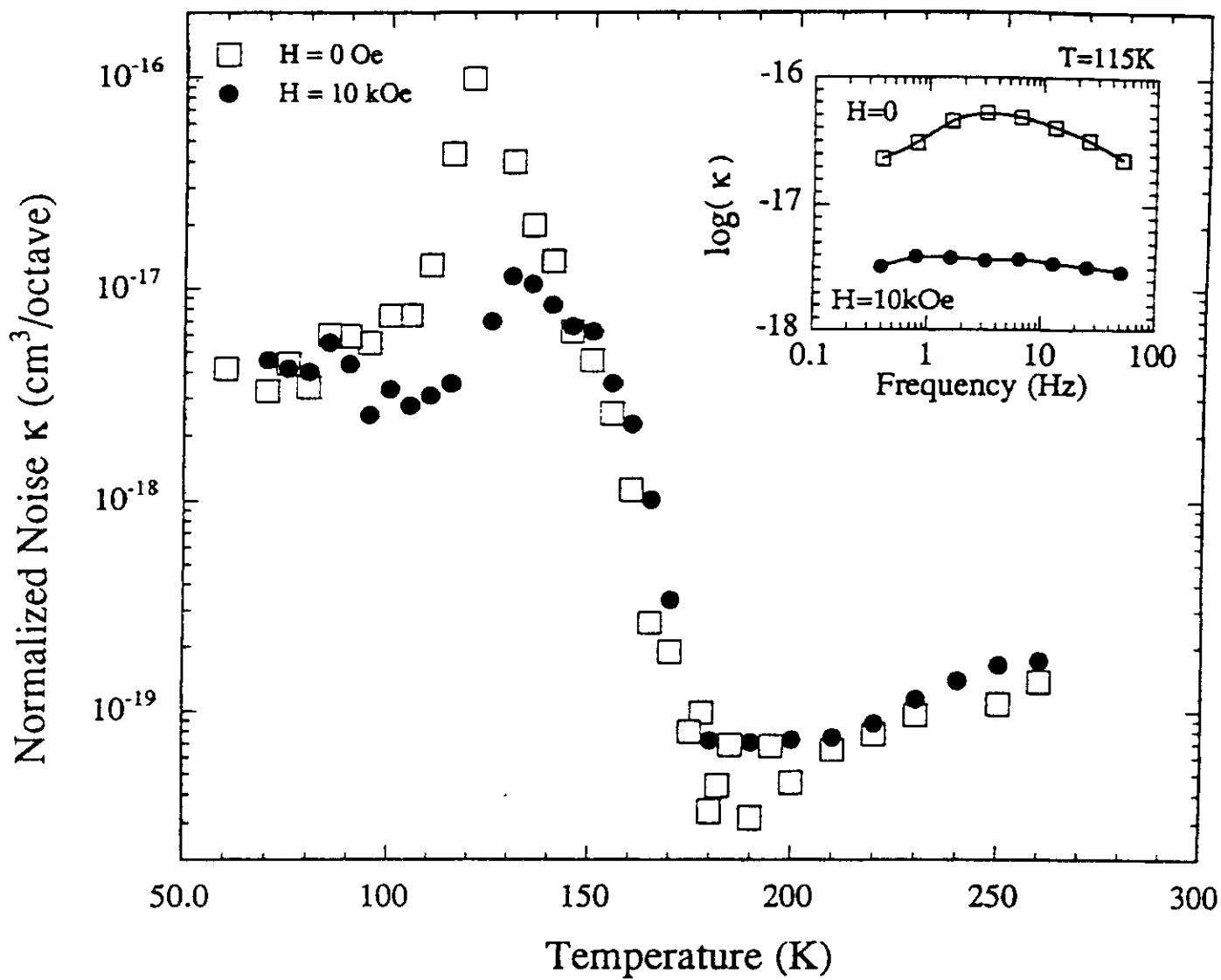
HEWLETT PACKARD LABORATORIES
THIN FILM DEPARTMENT
Jim Brug p950215

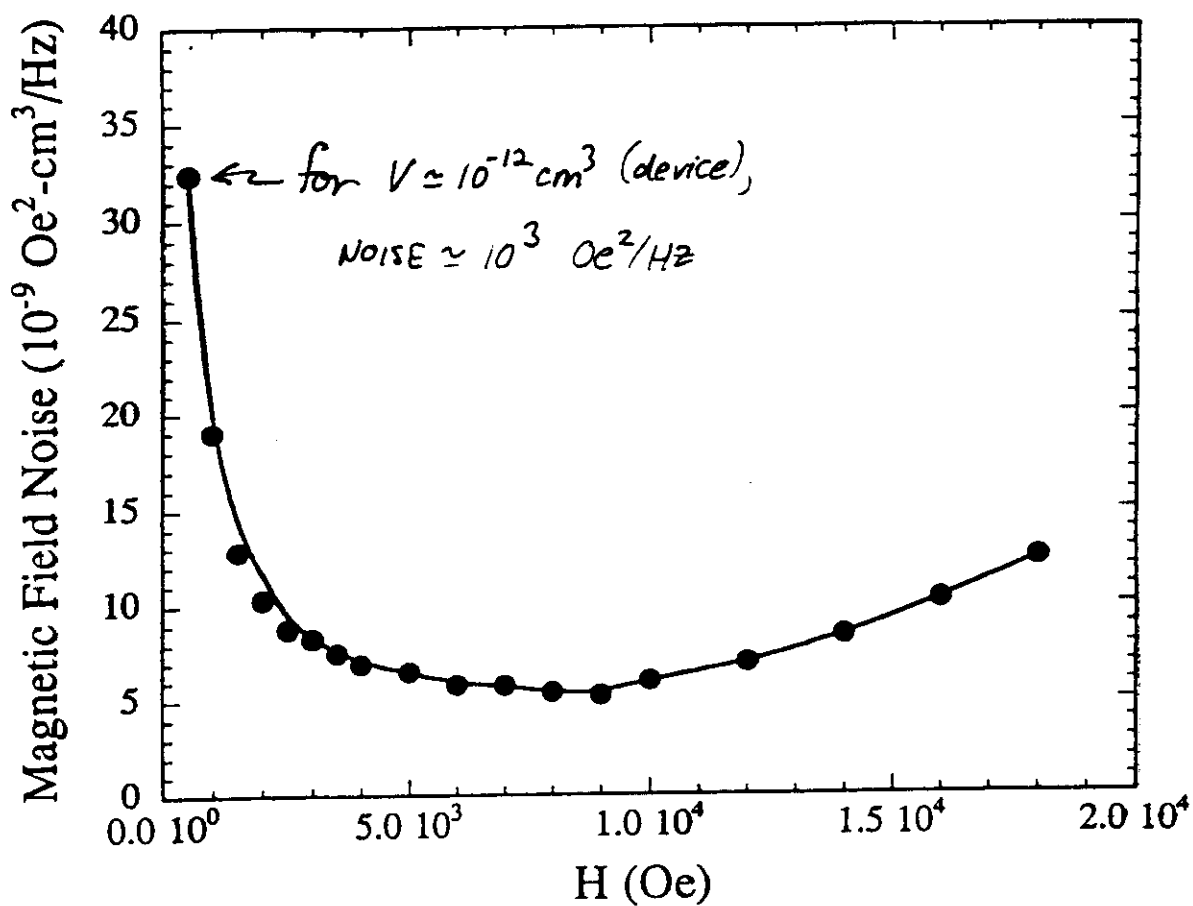


OPEN ISSUES

- low field MR - can CMR beat GMR?
- noise - Barkhausen-related noise at T_c ?
- microscopic mechanism
- new materials - alternatives to Mn-O perovskites?
- neighboring phases eg. charge order





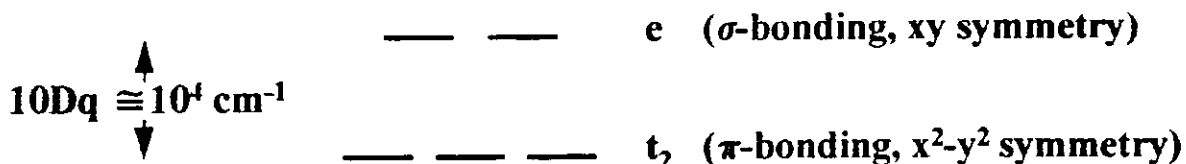


- Note, even field amplification might not help: $\text{Noise} \sim \text{MR} \sim \text{Magnetization}$.
- However, at high frequencies, and for reasonable power dissipation, a $10 \mu\text{m}^2$ device @ 10 MHz and $\partial R/\partial H \sim 10^{-4}$ detects a $\pm 1 \text{ Oe}$ signal with SNR of 20 dB! Good enough.

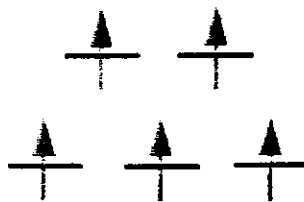
Single-ion properties of Mn - look at the d-electron series

19	20	21	22	23	24	25	26	27	28	29	30	31	32
K	Ca	Sc	Ti	V	Cr	Mn	Fe	Co	Ni	Cu	Zn	Ga	Ge
37	38	39	40	41	42	43	44	45	46	47	48	49	50

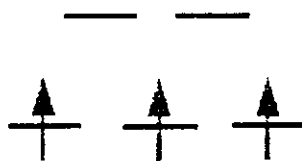
five crystal-field split d-states



$\text{Mn}^{2+} (d^5): S = 5/2, L = 0$

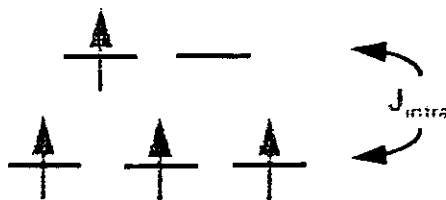


$\text{Mn}^{4+} (d^3): S = 3/2, L = 3$



Now for the case of Mn^{3+} - If $J_{\text{intra}} \approx 10 Dq$, then $S = 2, L = 2$. This assumption is based on acoustic paramagnetic resonance of Cr^{2+} ions in MgO.

$\text{Mn}^{3+} (d^4): S = 2, L = 2$



The acoustic paramagnetic resonance spectrum of chromous ions in magnesium oxide

F. G. MARSHALL† and V. W. RAMPTON

Department of Physics, University of Nottingham

MS. received 18th December 1967

Abstract. The acoustic paramagnetic resonance spectrum of the chromous ion as an impurity in magnesium oxide has tetragonal symmetry. There are three sets of chromous ions each giving a spectrum with its fourfold axis of symmetry along a $\langle 100 \rangle$ direction in the magnesium oxide. The three sets of ions can be aligned by the application of external uniaxial compression. The results are consistent with the chromous ion undergoing a dynamic Jahn-Teller effect and there being a distortion from cubic symmetry at each chromous ion site due to random internal strains in the crystal.

The Jahn-Teller effect of octahedrally co-ordinated $3d^4$ ions

J. R. FLETCHER and K. W. H. STEVENS

University of Nottingham

MS. received 26th July 1968

Abstract. The chromous ion in magnesium oxide is studied and an interpretation is given of the acoustic paramagnetic resonance results of Marshall and Rampton. Because of the very strong orbit-lattice interaction it is important to take full account of the Jahn-Teller effect. The cluster approximation justified previously is used, and then are added the spin-orbit coupling, anharmonic forces, external magnetic field and random lattice strains. The resultant secular equations are usually solved numerically in terms of parameters to describe the strains and anharmonic couplings. It is postulated that the observed line shapes reflect random strain distributions and that peaks in the lines are correlated with turning points in the strain-resonance field curves. Parameters are chosen to fit the observations for a definite field orientation and it is shown that a good interpretation can then be given for the results for a variety of orientations. The energy-level diagram of the chromous ion is shown to be quite complicated, and it is pointed out that many more transitions than have yet been observed can be expected.

$$\mathcal{H}_1 = \frac{1}{2M_0}(P_2^2 + P_3^2) + \frac{1}{2}M_0\omega_D^2(Q_2^2 + Q_3^2) + BQ_3(Q_3^2 - 3Q_2^2) \quad \text{Elastic}$$

$$\mathcal{H}_2 = 2\epsilon(T_1Q_3 + T_2Q_2) \quad \text{Jahn-Teller}$$

$$\mathcal{H}_3 = 2D\{T_1(S_z^2 - 2) + \sqrt{\frac{1}{3}}T_2(S_z^2 - S_y^2)\} \quad \text{zero-field splitting}$$

$$\mathcal{H}_4 = (2 - 4\mu)\beta H \cdot S + 4\mu\beta\{T_1(2H_zS_z - H_xS_x - H_yS_y) + \sqrt{3}T_2(H_xS_x - H_yS_y)\} \quad \text{Zeeman}$$

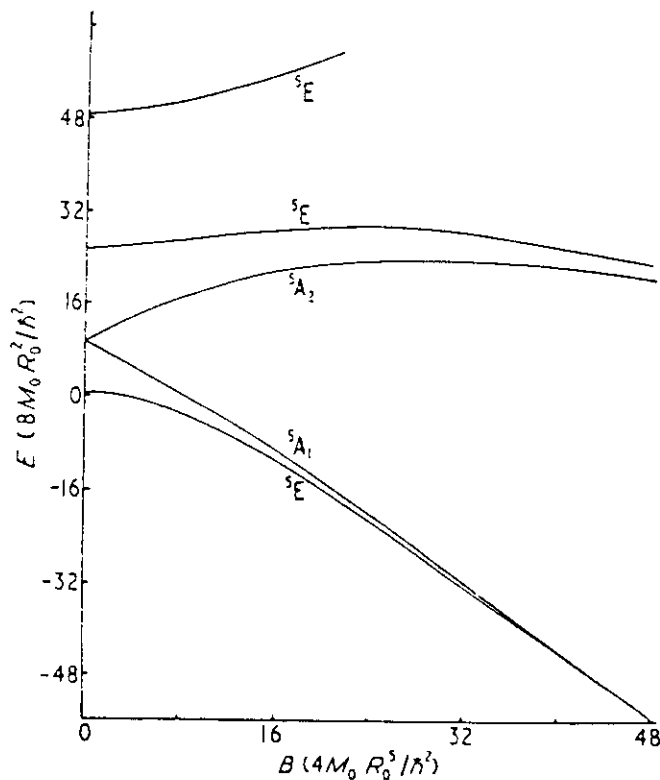


Figure 1. Energy levels of the complex neglecting spin degeneracy.

Table 3. Values of parameters for Cr²⁺ in MgO

Symbol		
ω_D	longitudinal optical phonon frequency	$9.2 \times 10^{13} \text{ s}^{-1}$
λ	spin-orbit coupling parameter	57 cm^{-1}
ϵ	Jahn-Teller coupling coefficient	$3.6 \times 10^{-9} \text{ J m}^{-1}$
B	anharmonic force constant	$1.88 \times 10^{12} \text{ J m}^{-3}$
D	zero-field splitting constant	2.02 cm^{-1}
R_0	Jahn-Teller displacement	$1.6 \times 10^{-11} \text{ m}$
δ	tunnelling splitting	7.6 cm^{-1}
K	acoustic coupling coefficient	$4.4 \times 10^{-19} \text{ J}$
a	MgO nearest-neighbour distance	$2.1 \times 10^{-10} \text{ m}$
e	local tetragonal strain	varies between specimens
	$=\epsilon_{zz} - \frac{1}{2}(\epsilon_{xx} + \epsilon_{yy})$	$\sim -2 \times 10^{-5}$

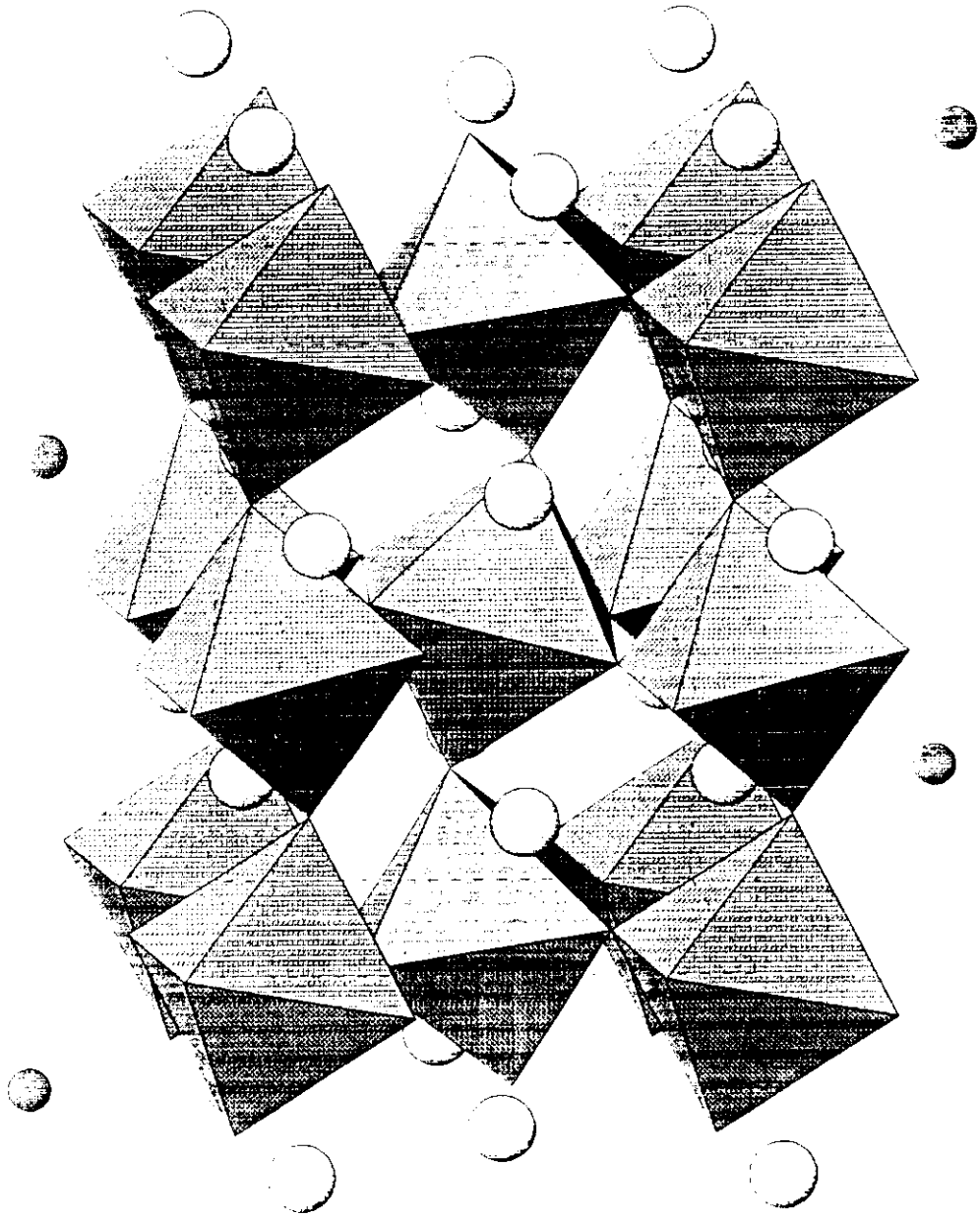
Fletcher + Stephens '69

LaMnO₃ crystal structure

yellow = La

blue = MnO₆ octahedra

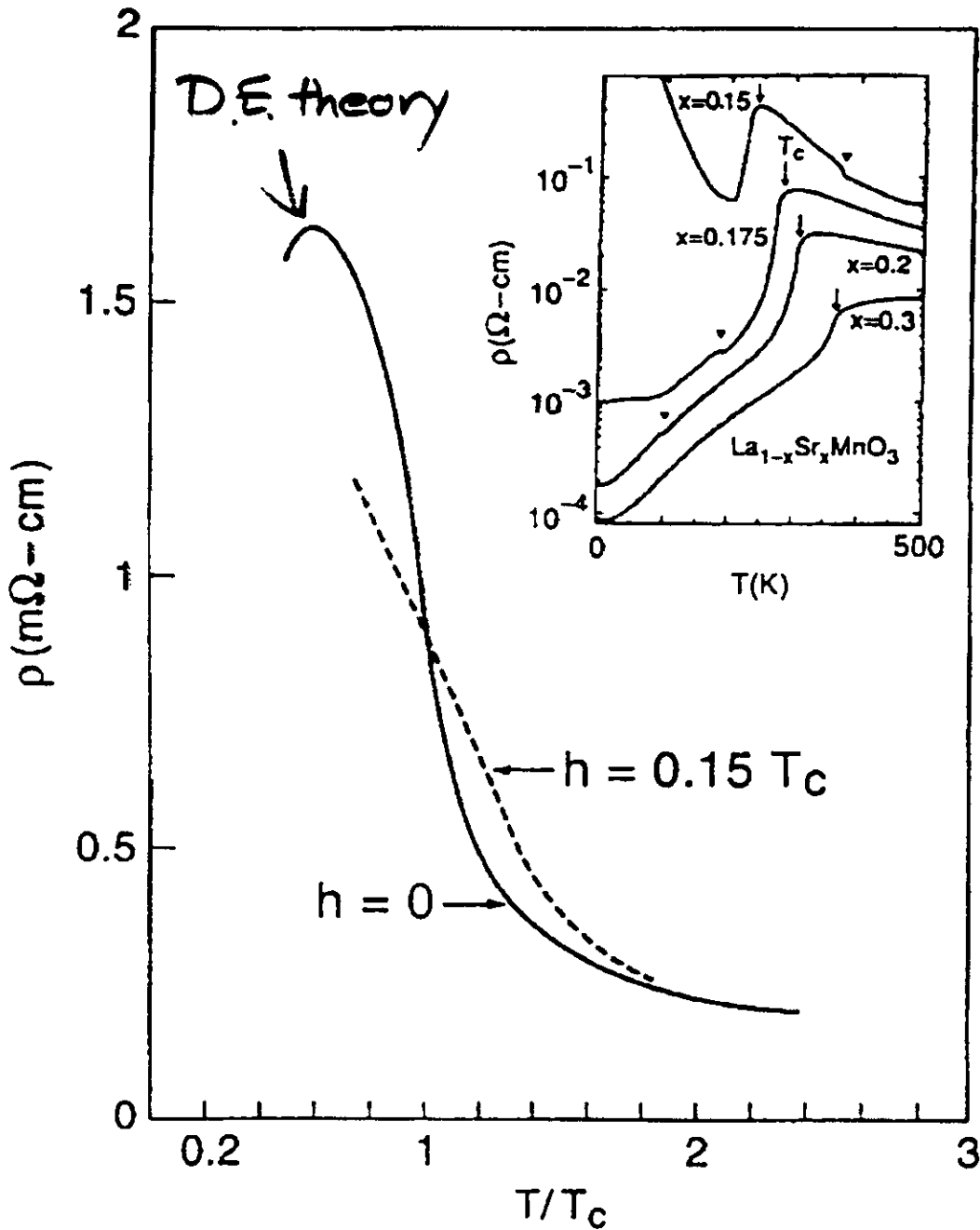




Limitations of a description in terms of Double Exchange alone.

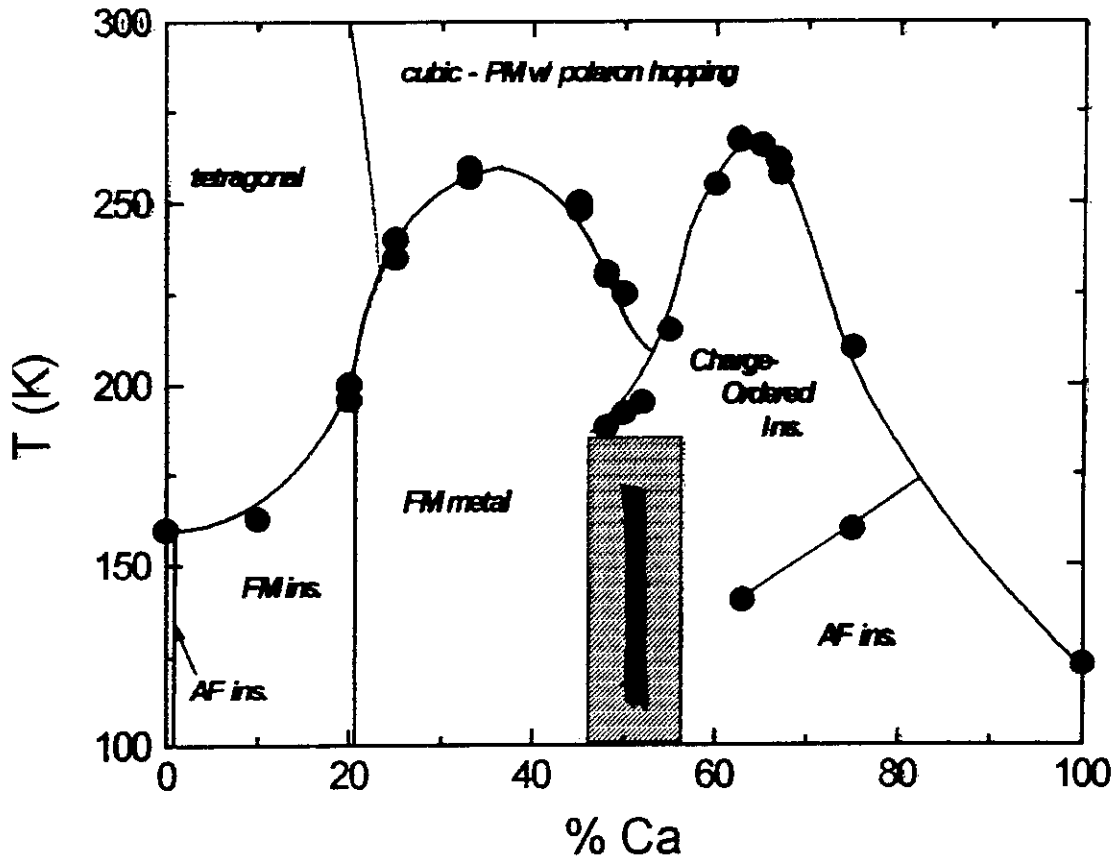
Millis, Littlewood & Shraiman (1995)

(Resistivity data of Tokura et al.)

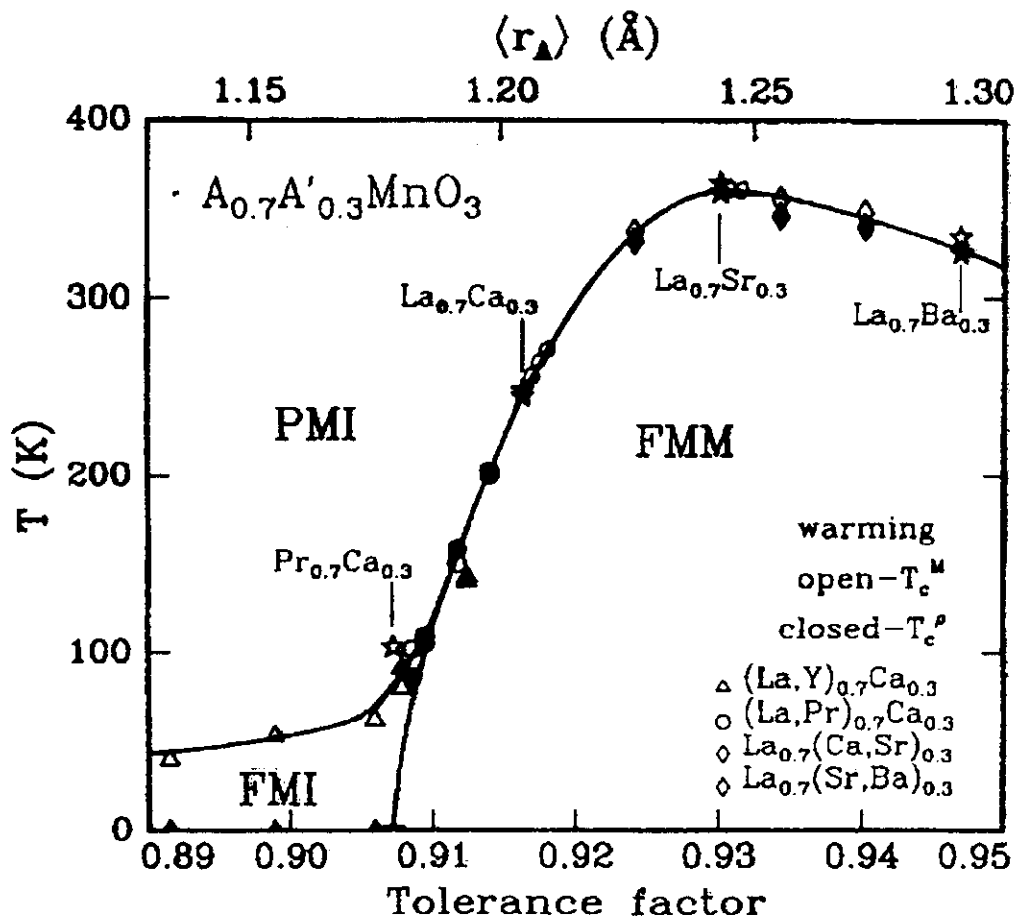
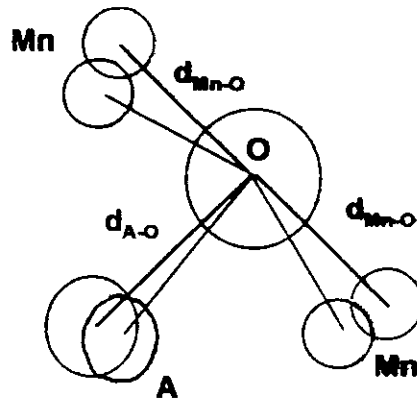


- ρ_{theory} too low
- wrong h -dependence, $T (< T_c)$ dependence
- MLS \rightarrow polaron effects

Revised Phase Diagram - $\text{La}_{1-x}\text{Ca}_x\text{MnO}_3$

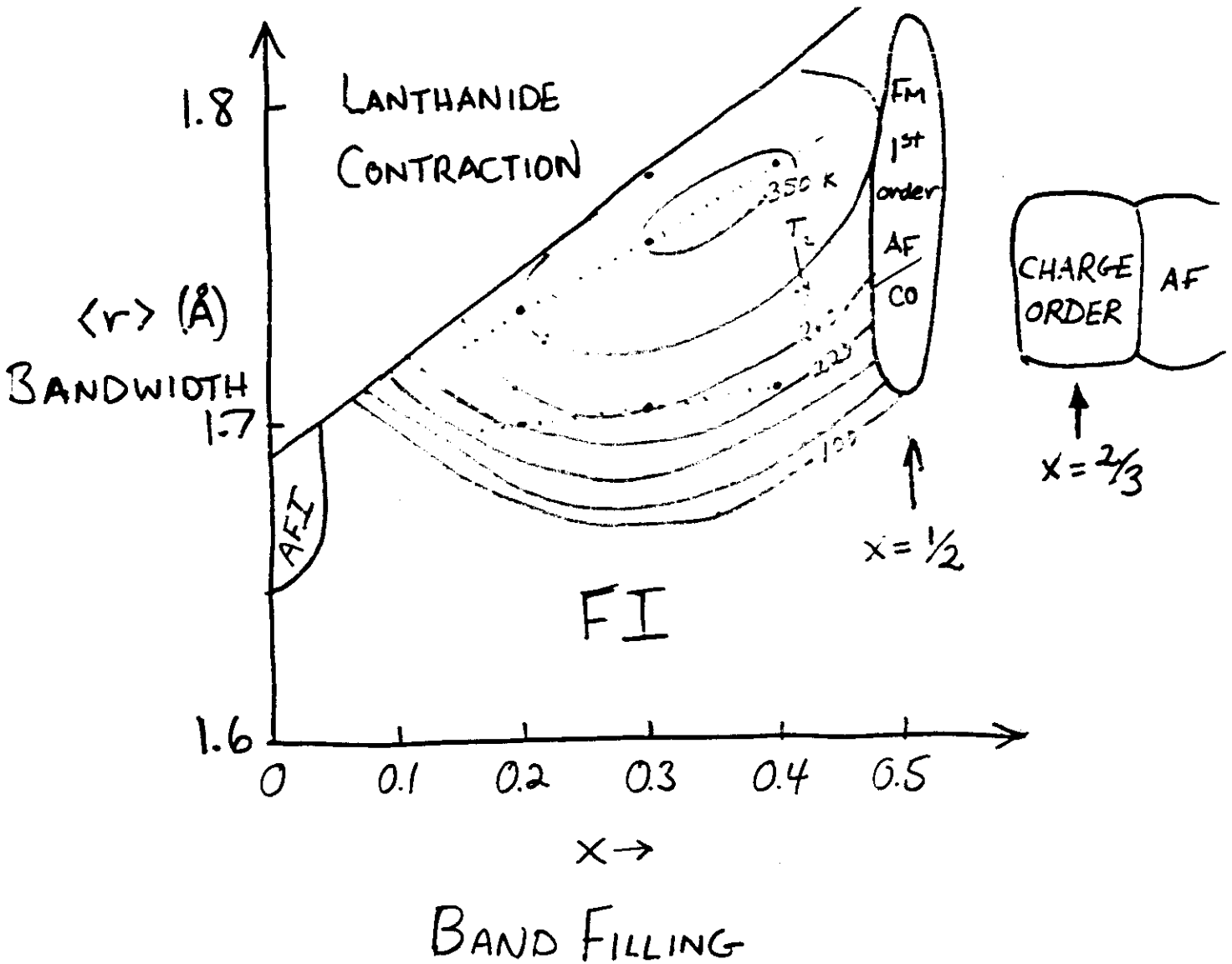


Here $\langle r_A \rangle$ is the "A" site radius. Result that T_c decreases and ρ increases as $\langle r_A \rangle$ decreases in CMR regime means hopping is not through 180° bonds, but rather at an angle governed by the "tolerance factor" = $t = (d_{A-O})/\sqrt{2}(d_{Mn-O})$.
 •Applied pressure does the same as chemical pressure.



DOPED MANGANITE PEROVSKITE

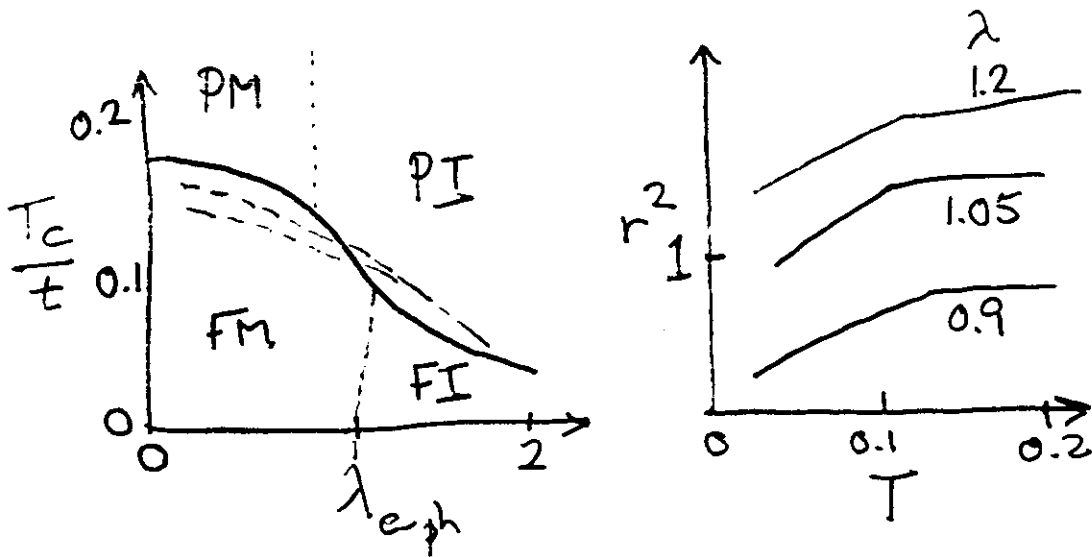
GROUND STATES

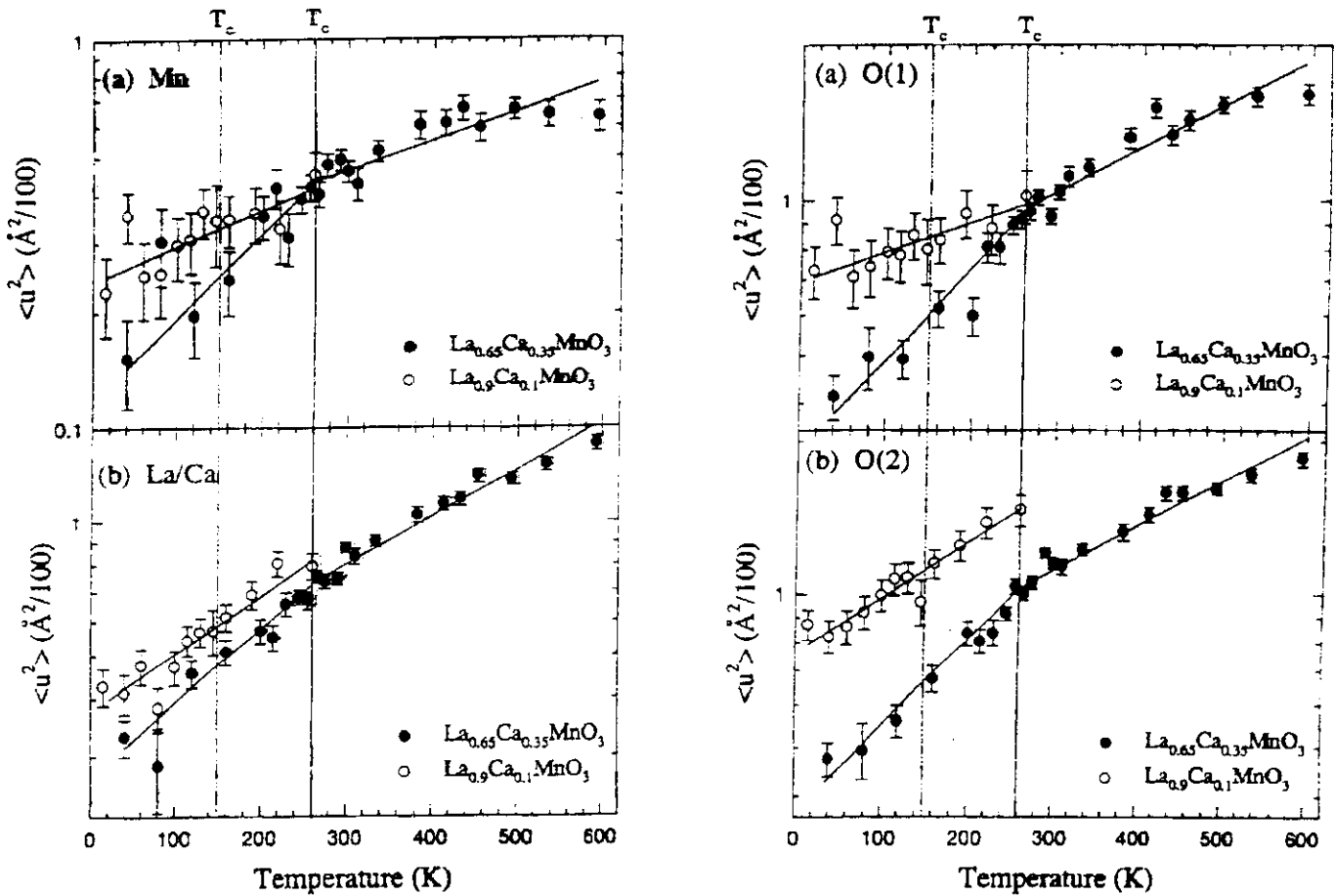


THEORY SUMMARY (Millis, Shraiman + Mueller)

Approximations

- large Hund's energy
- e-ph coupling to on-site harmonic phonons
- neglect U .
- spins, phonons classical
- $d \rightarrow \infty$ ("dynamical MFT" ala G, K, KR)





neutron cross section $\sigma \propto e^{-2W}$; $2W(\vec{Q}) = \langle (\vec{Q} \cdot \vec{u})^2 \rangle$
 $\langle u^2 \rangle = \text{rms displacements}$

Gruneisen coeff: $\gamma \sim \frac{\partial \ln \omega}{\partial V}$

$$W(T) \propto [V(T)]^{2\gamma}$$

$\langle u^2 \rangle$ Data $\Rightarrow \gamma \sim 85!$; not due to volume expansion

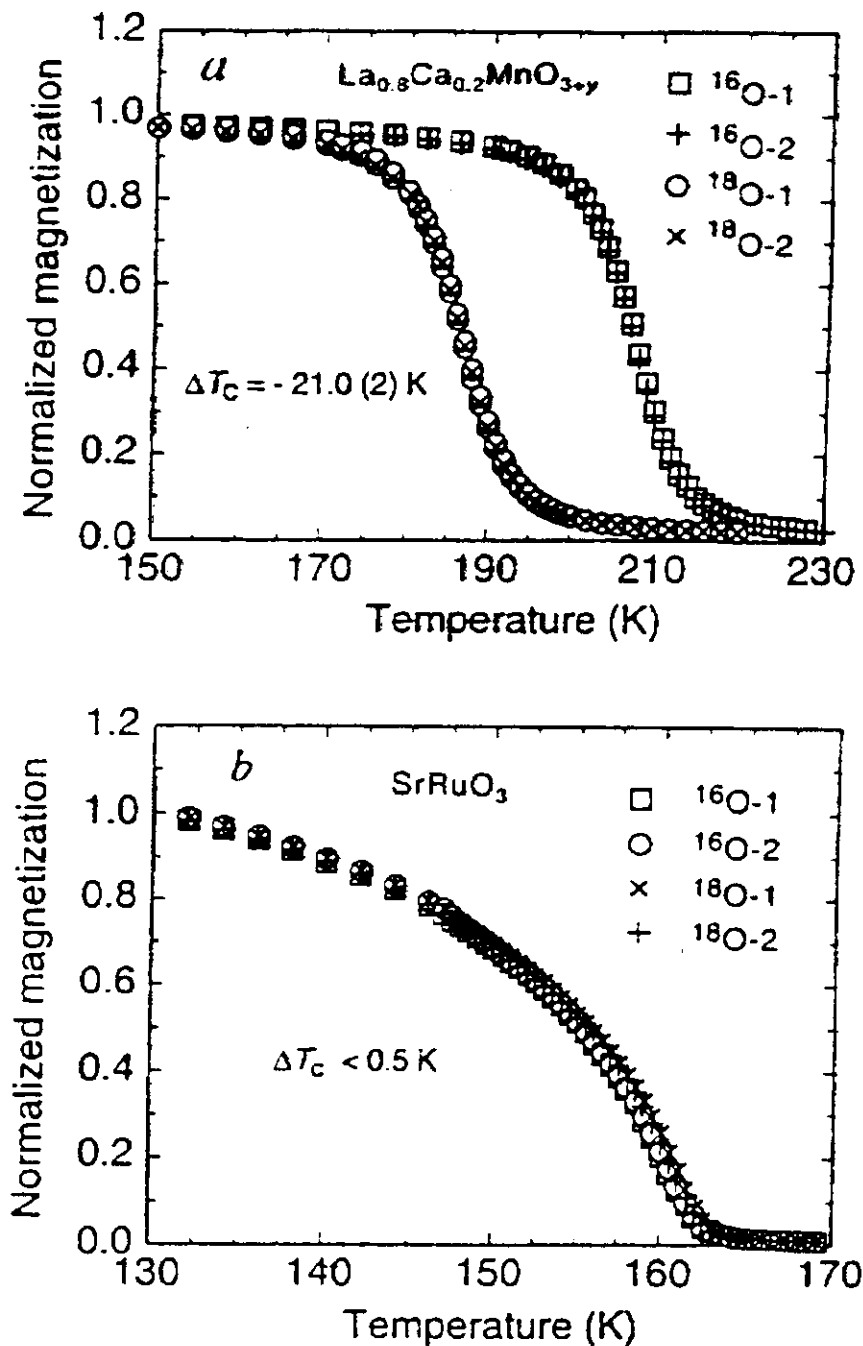
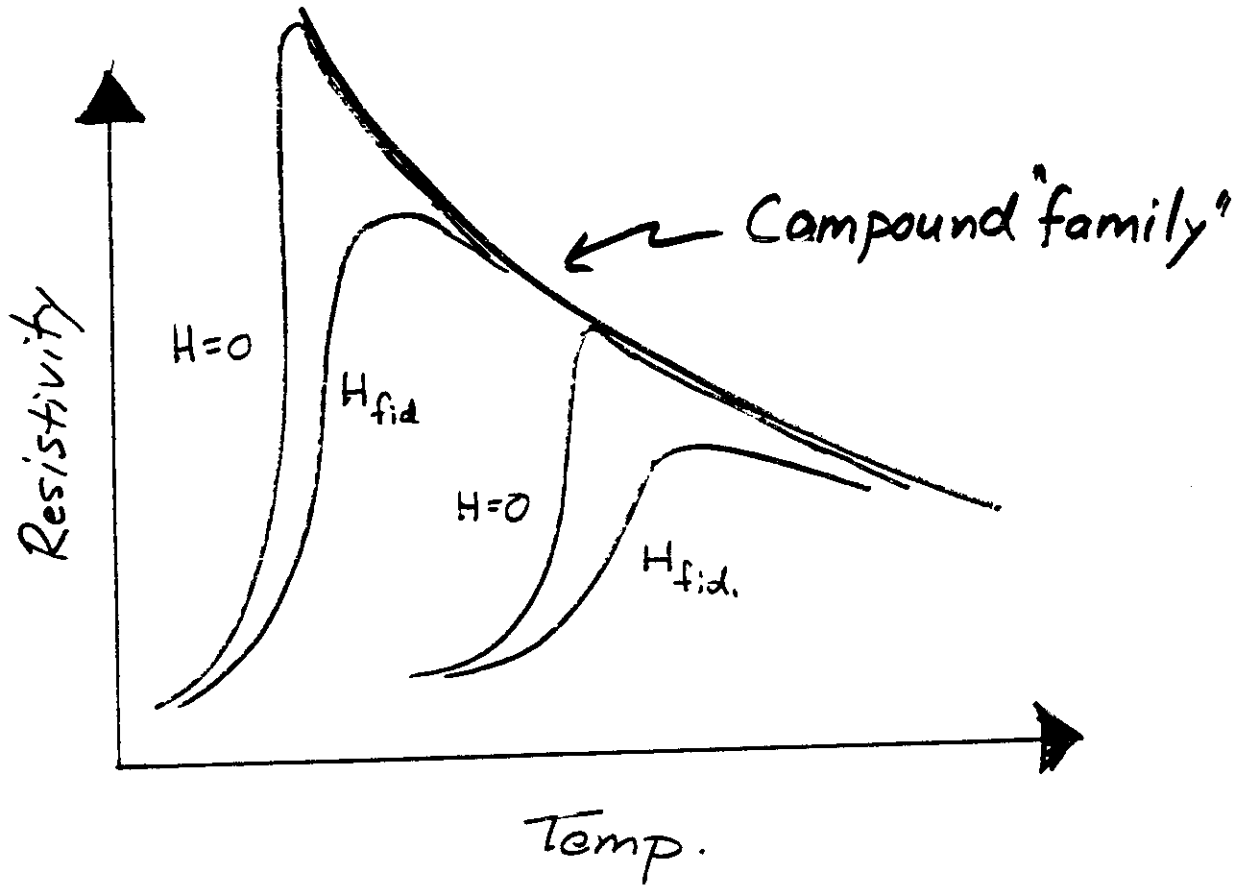
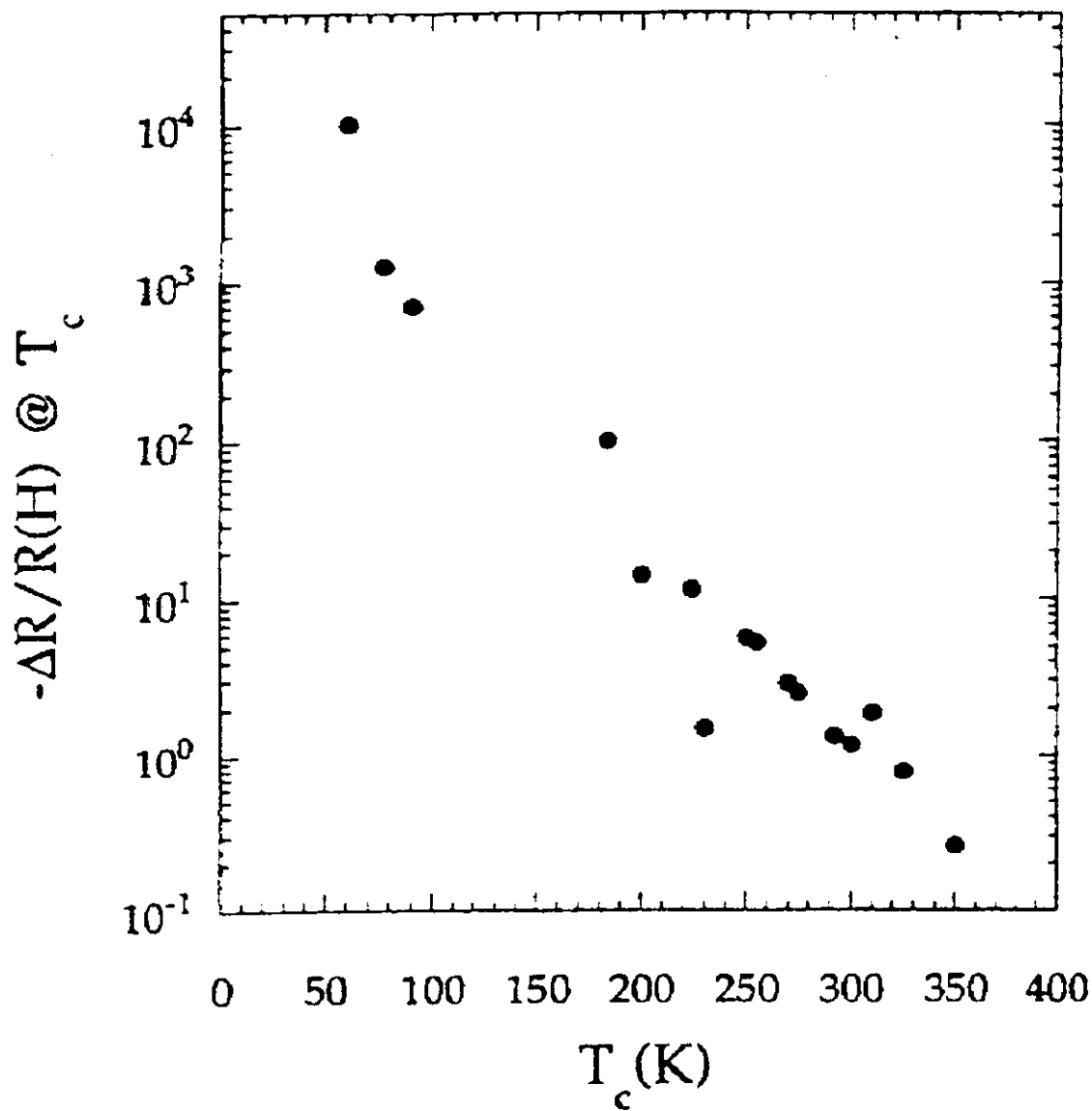


FIG. 1 Oxygen isotope effect on the Curie temperature of $\text{La}_{0.8}\text{Ca}_{0.2}\text{MnO}_{3-y}$ and SrRuO_3 : temperature dependence of the normalized magnetization for ^{16}O and ^{18}O samples of $\text{La}_{0.8}\text{Ca}_{0.2}\text{MnO}_{3-y}$ (a) and SrRuO_3 (b). There is a large oxygen isotope effect on Curie temperature ($\sim 21 \text{ K}$) in $\text{La}_{0.8}\text{Ca}_{0.2}\text{MnO}_{3-y}$ with a strong JT effect, but no observable effect in the ferromagnet SrRuO_3 with a negligible JT effect. Note that the two independent ^{16}O samples (as well as the two independent ^{18}O samples) have the same T_c , demonstrating an excellent reproducibility of the isotope experiments.

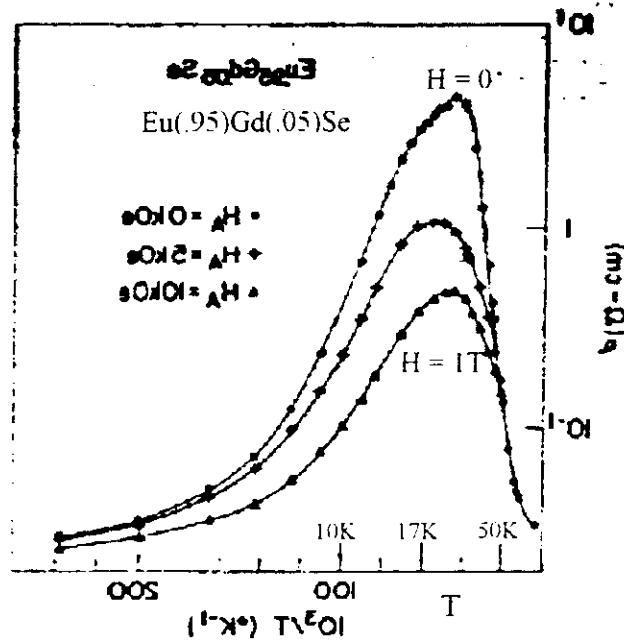
THE basic effect



$A_{1-x}B_xMnO_3$



- CMR in manganite perovskites has:
 - heterovalency, Mn^{3+}/Mn^{4+} pairs \rightarrow double exchange
 - large Jahn-Teller effect from Mn^{3+}
- However, other compounds exhibit CMR especially at low T, e.g.



von Molnar & Methfessel

- Want other systems with CMR but at higher T.

Look at the pyrochlore structure family, $Tl_2Mn_2O_7$

- MnO_6 octahedra in tetrahedral coordination
- Ferromagnetic (Greedan)
- Conducting
- CMR exhibited (Shimakawa, Kubo & Manako)

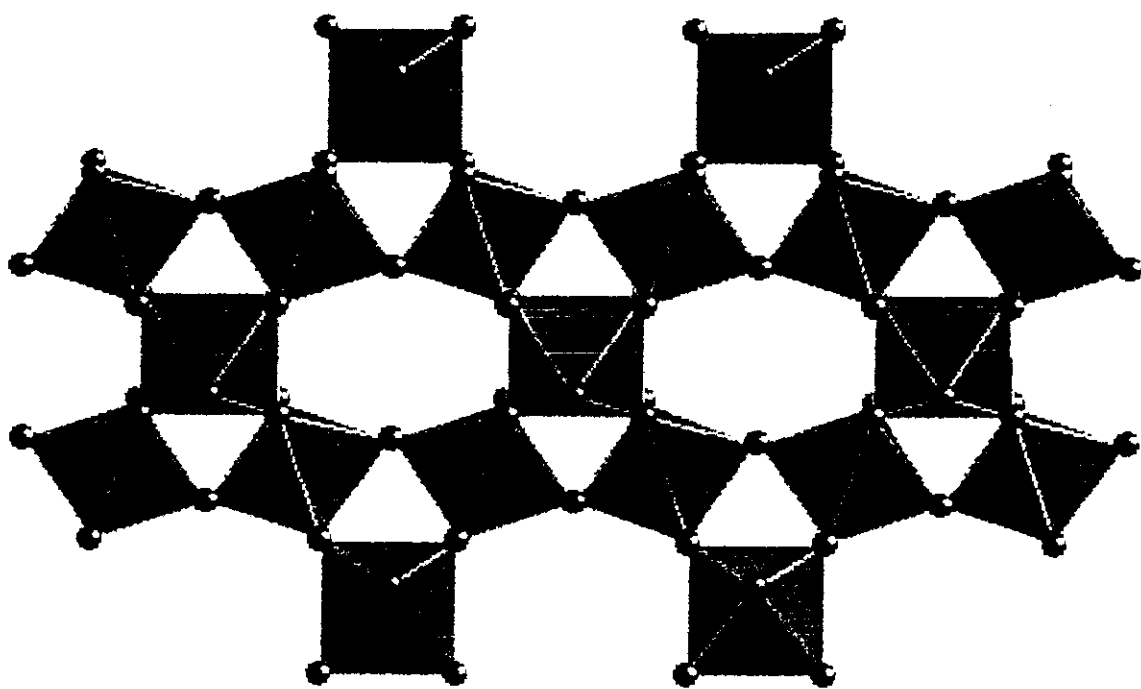
Differences with perovskites $La_{1-x}Ca_xMnO_3$

$Tl_2Mn_2O_7$ is:

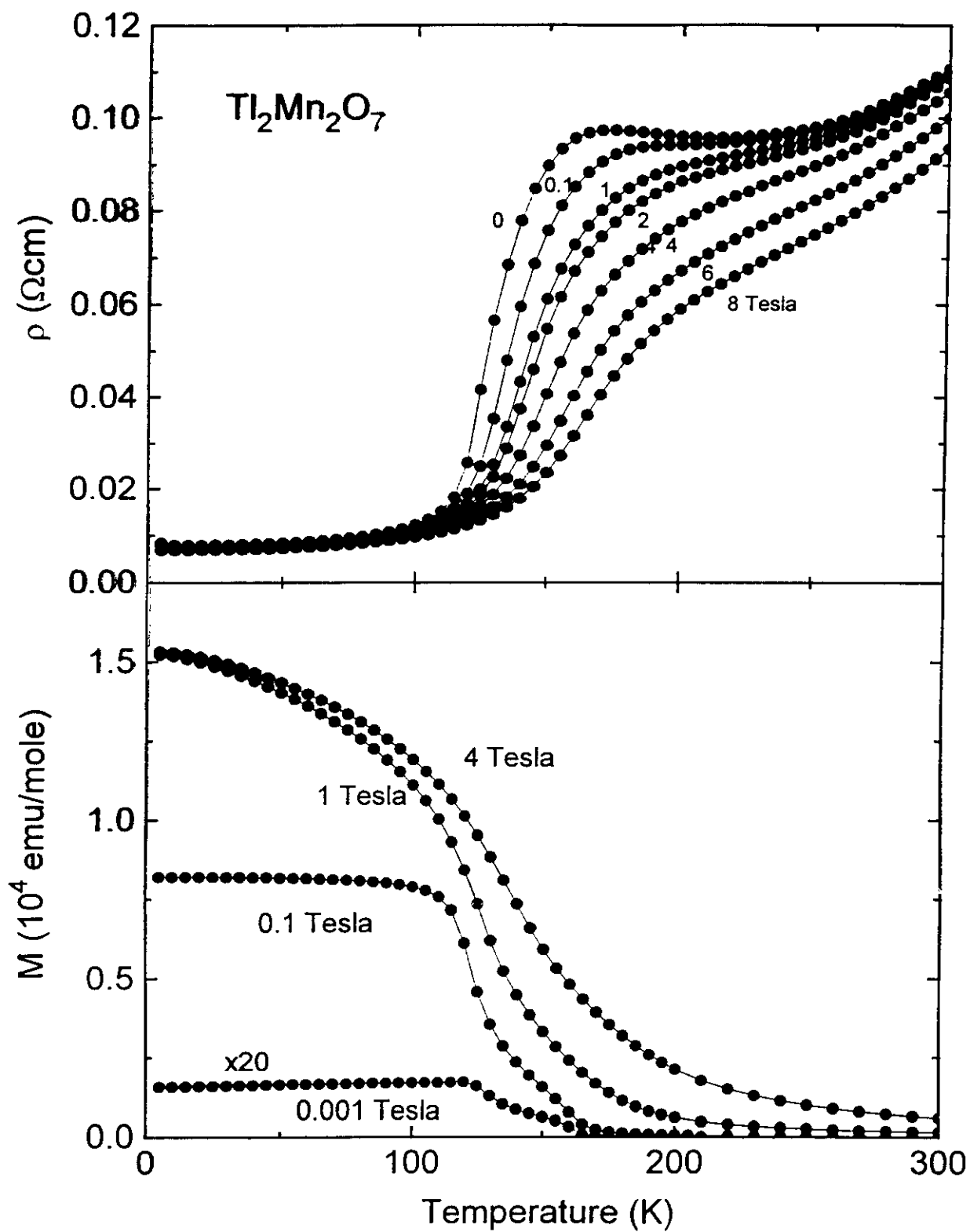
- Almost stoichiometric
- \therefore No Jahn-Teller ion
- Tl bands near the Fermi level—possibly important for conduction
- Mn-O-Mn angle much more acute (134°) than in perovskites.

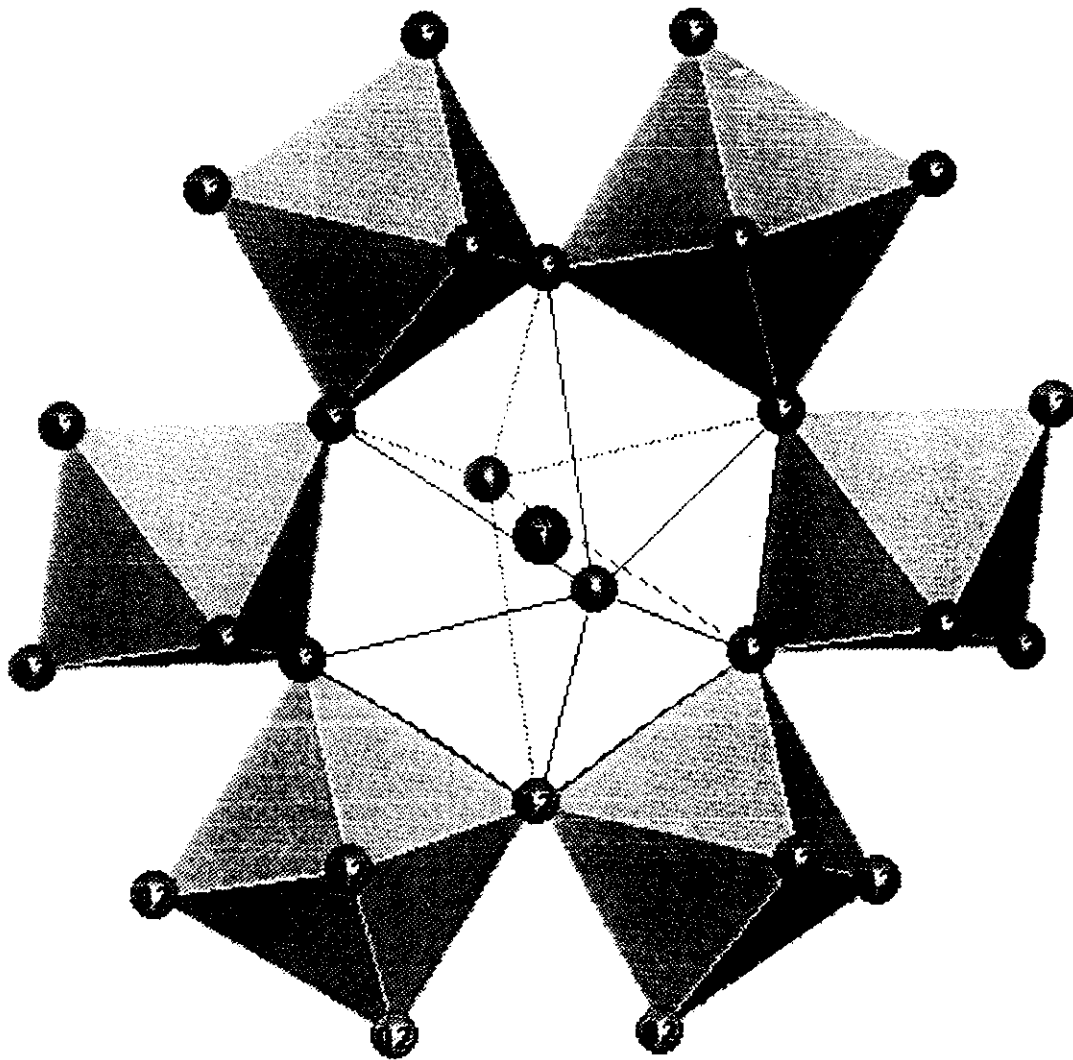
Need to know stoichiometry **PRECISELY**—no obvious source of Double Exchange from nominal composition.

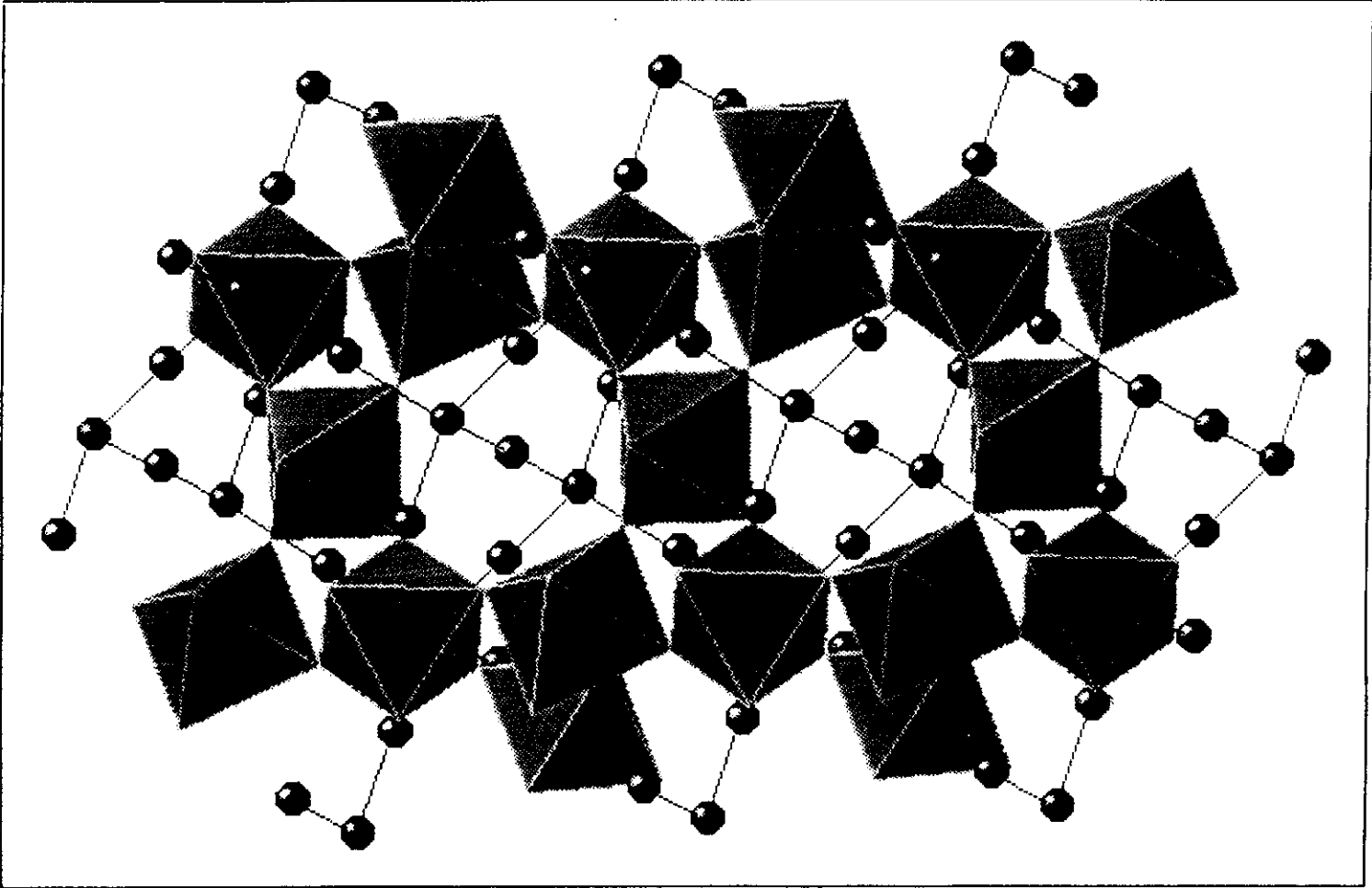
- Neutron Powder Diffraction
- Single crystal x-ray diffraction

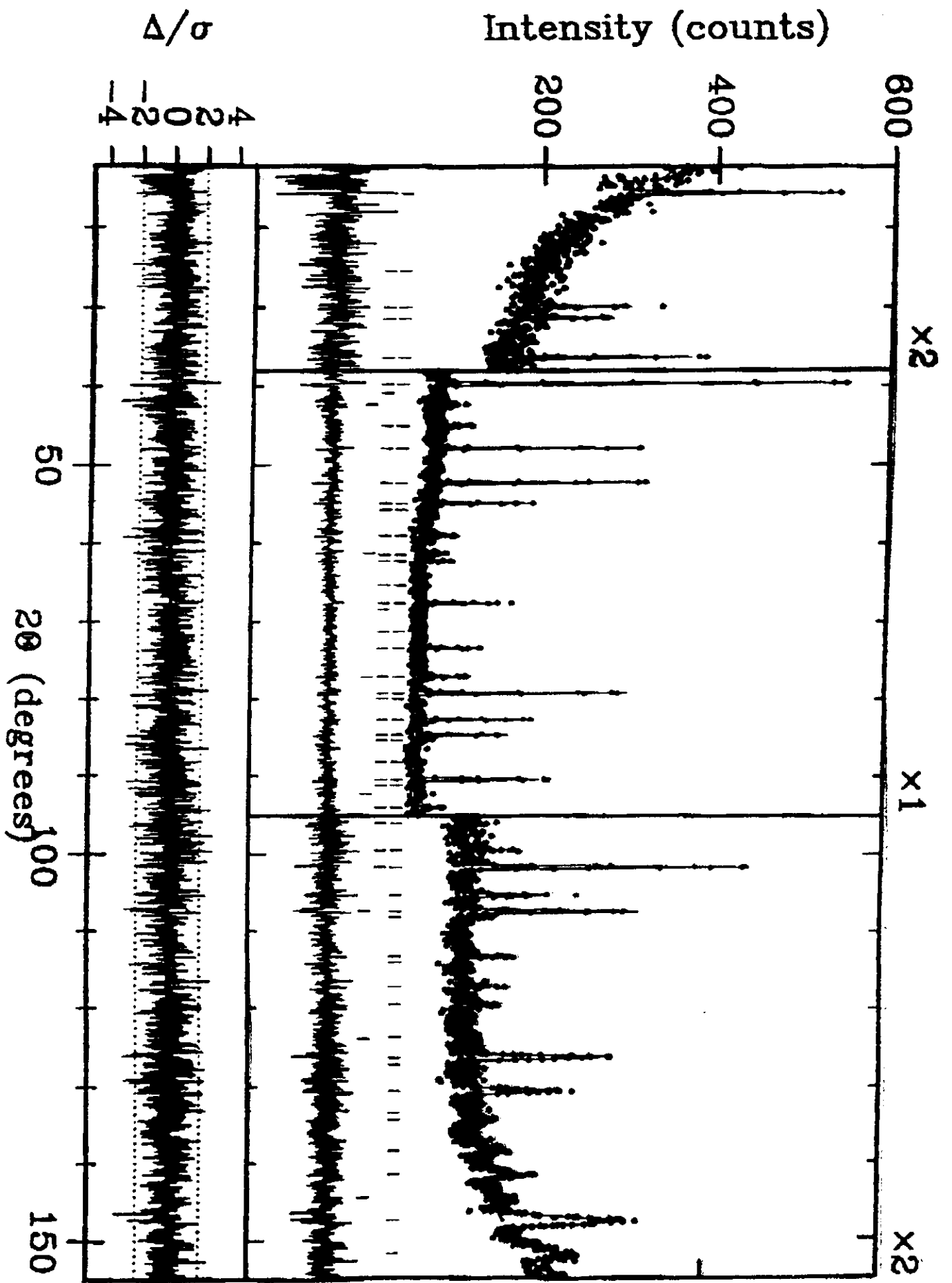


MnO_6 octahedral network in $\text{Tl}_2\text{Mn}_2\text{O}_7$
[Mn_2O_6]









Summary & Conclusions

- Stoichiometry of $\text{Tl}_2\text{Mn}_2\text{O}_7$ accurate to 0.5% (Tl) and 2.5% (O)
- Saturation moment $2.74 < 3$ (Mn^{4+}). Consistent with no Mn^{3+} .
- No Jahn-Teller distortion of Mn-O₆ octahedra observed.
- Transport consistent w/ metallic state above T_c .

Perovskites:

Same mechanism (Double Exchange) driving the FM ordering as leading to metallic conductivity.

Tl-pyrochlores:

FM ordering driven by superexchange between Mn^{4+} .

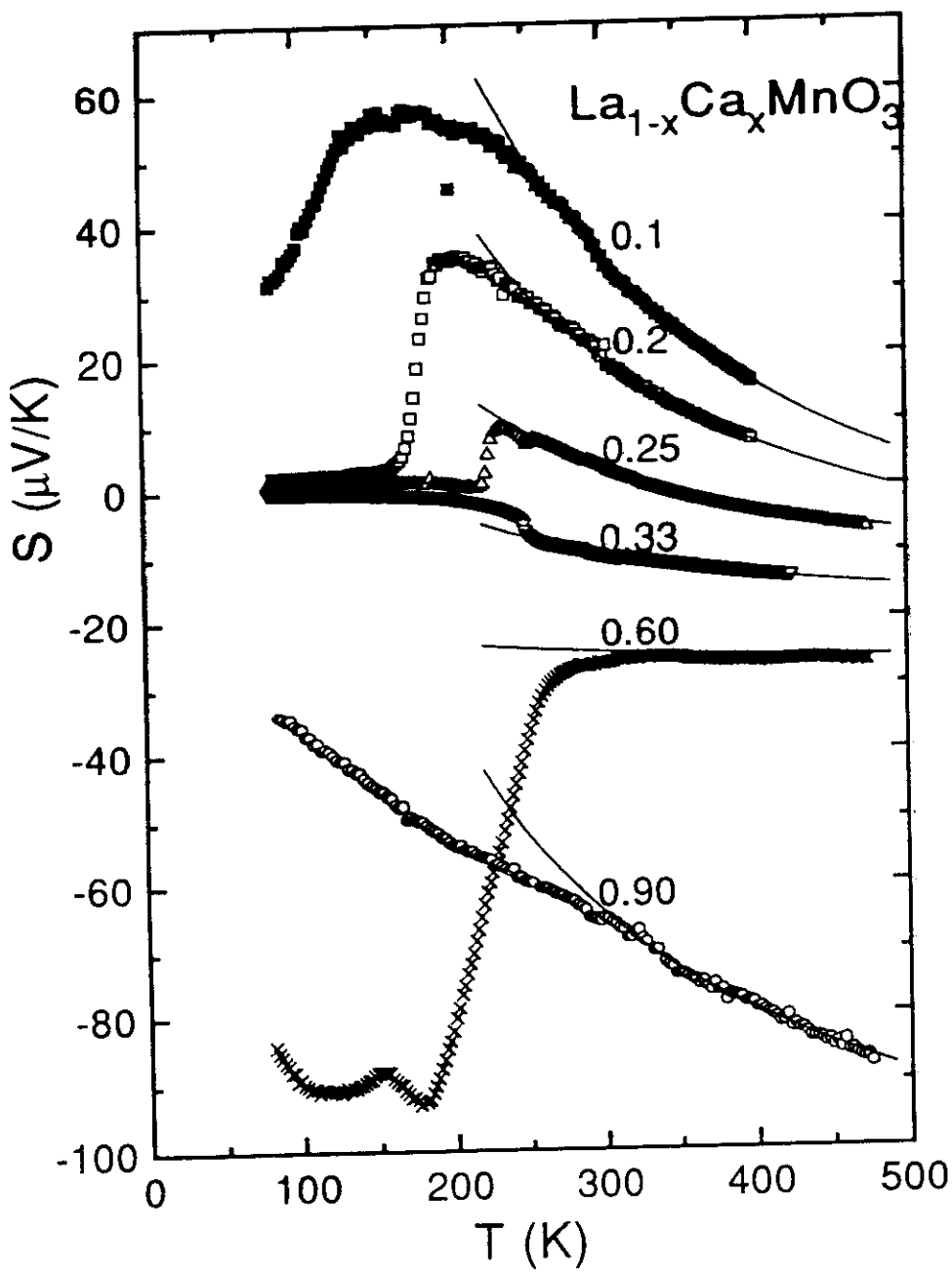
Metallic conduction from the Tl-O sublattice.

Strong incoherent spin-fluctuation scattering by Mn^{4+} spins.

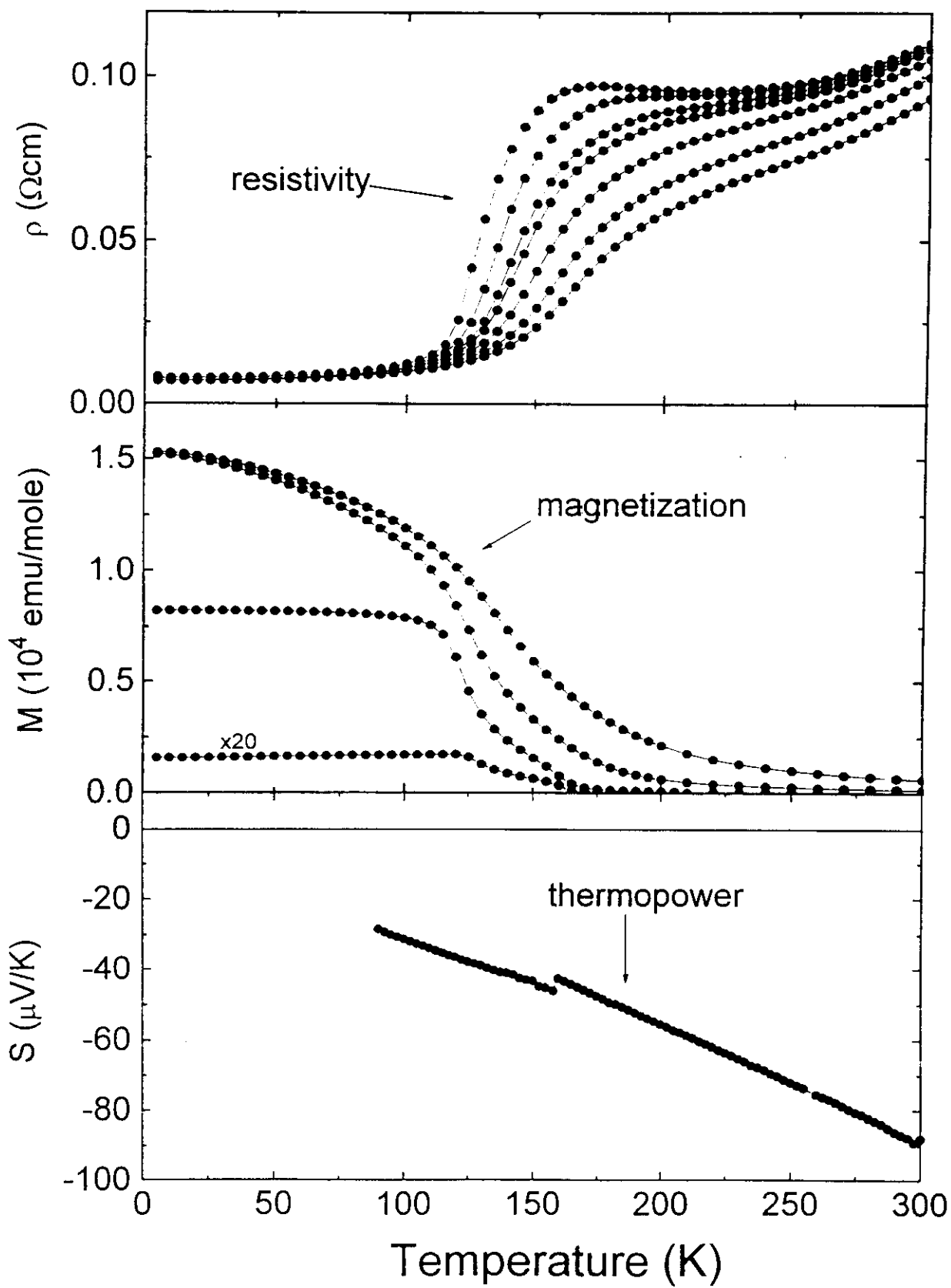
CMR from dT_c/dH .



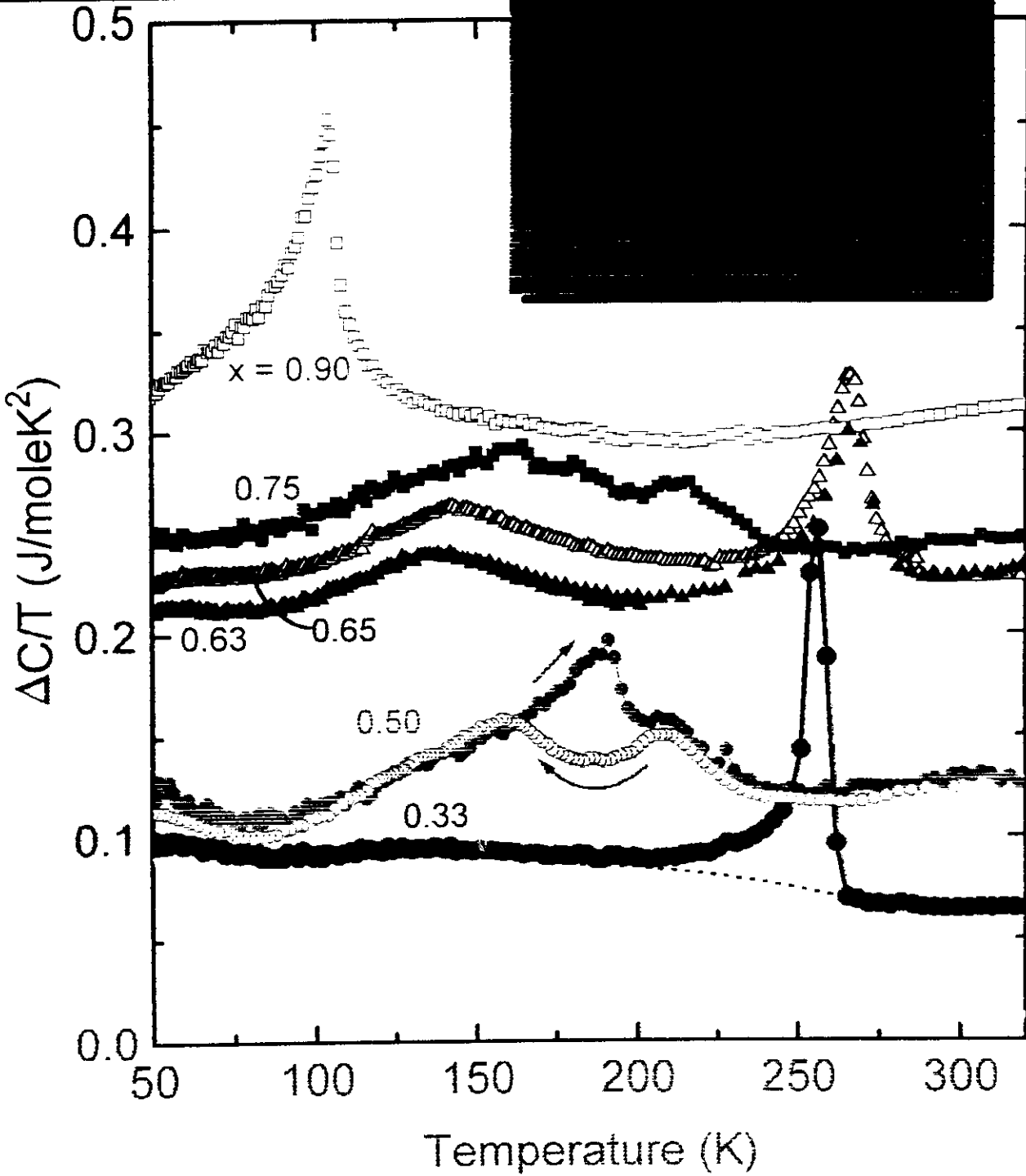
CMR in the pyrochlores broadens the search for new CMT compounds.



$\text{Tl}_2\text{Mn}_2\text{O}_7$



**High Temperature
Specific Heat - $\text{La}_{1-x}\text{Ca}_x\text{MnO}_3$**



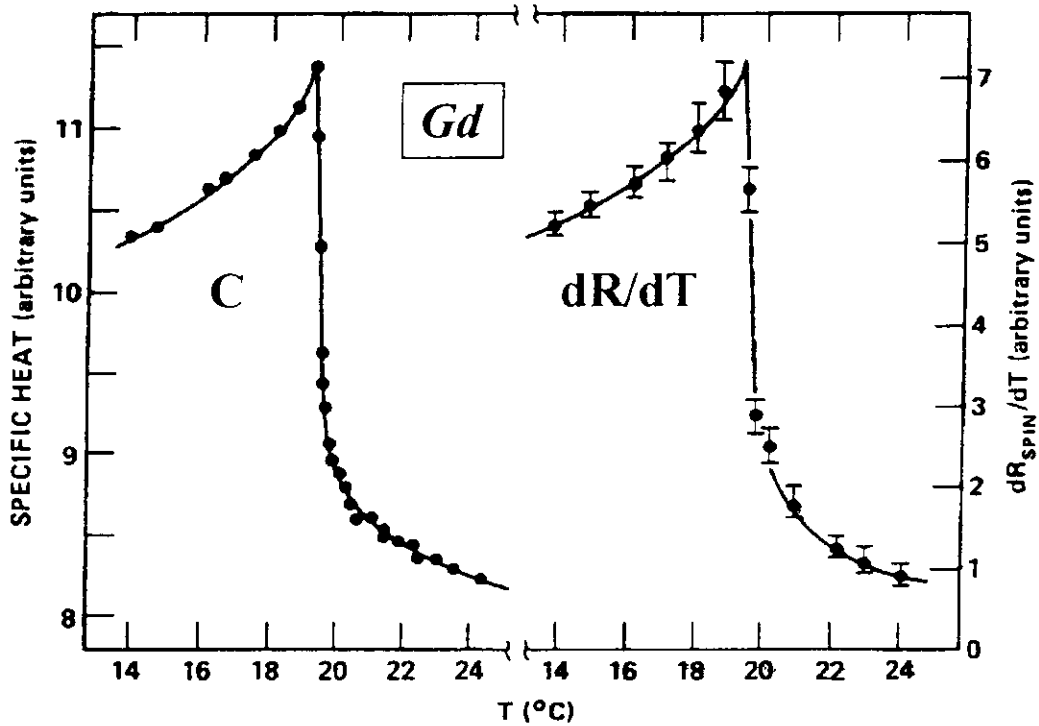
How is the resistance change in $La_{1-x}Ca_xMnO_3$ uncommon?

For $\rho = m/ne^2\tau$, Langer and Fisher (1968) calculate τ in the presence of magnetic fluctuations. For $T > T_c$, relaxation rate:

$$\tau^{-1} \propto \text{magnetic energy}$$

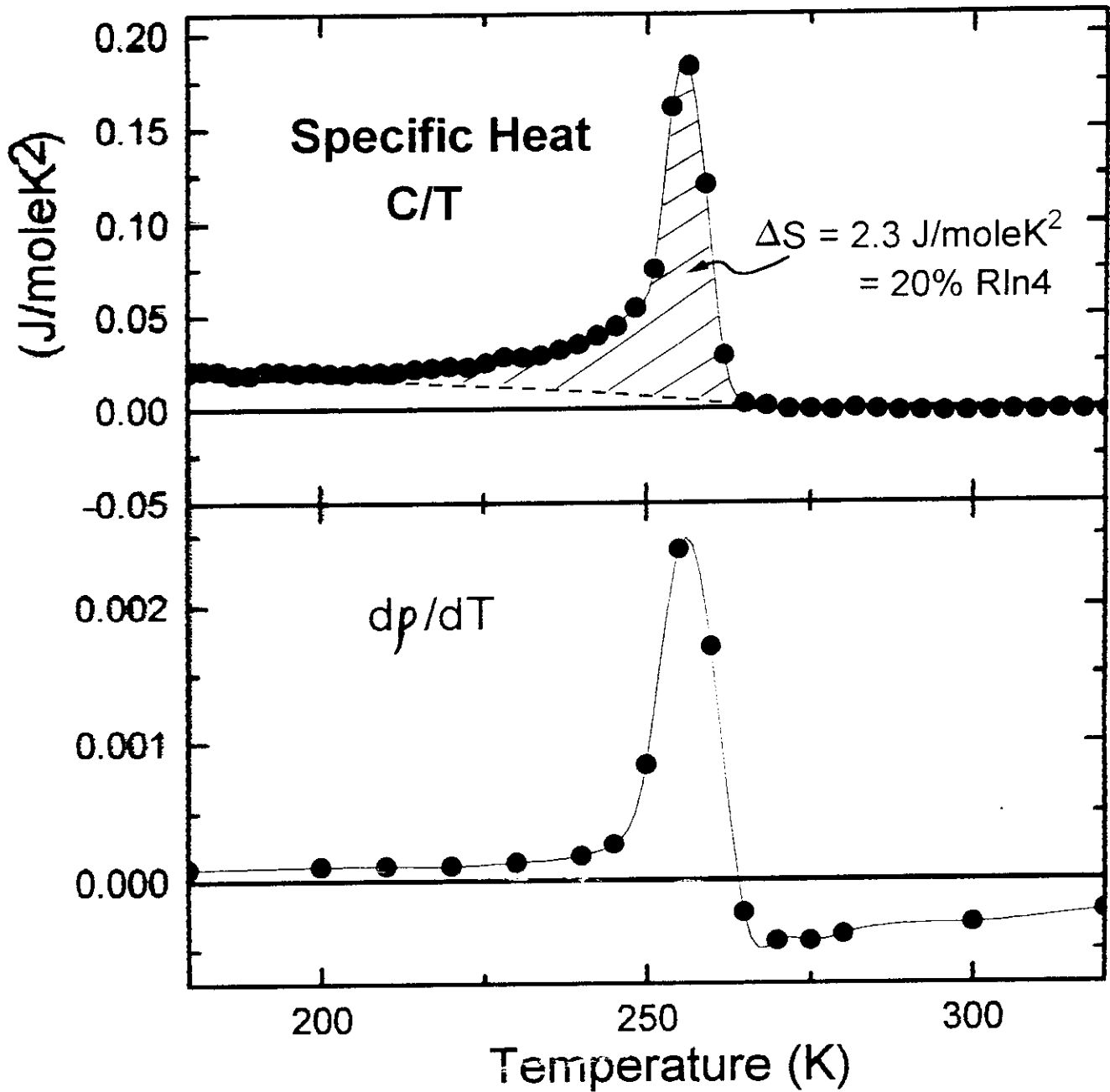
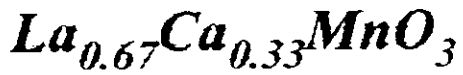


$$C \propto dR/dT$$



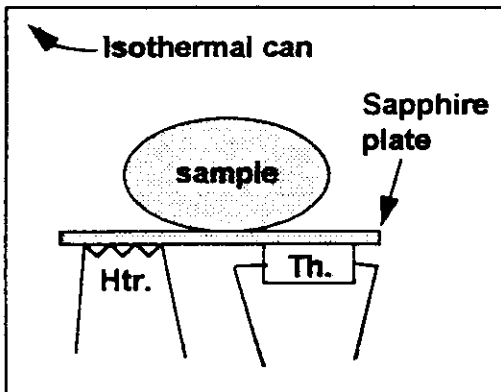
after Parks (1971)

Compare Spec. Ht. to Resistance ala Langer-Fisher

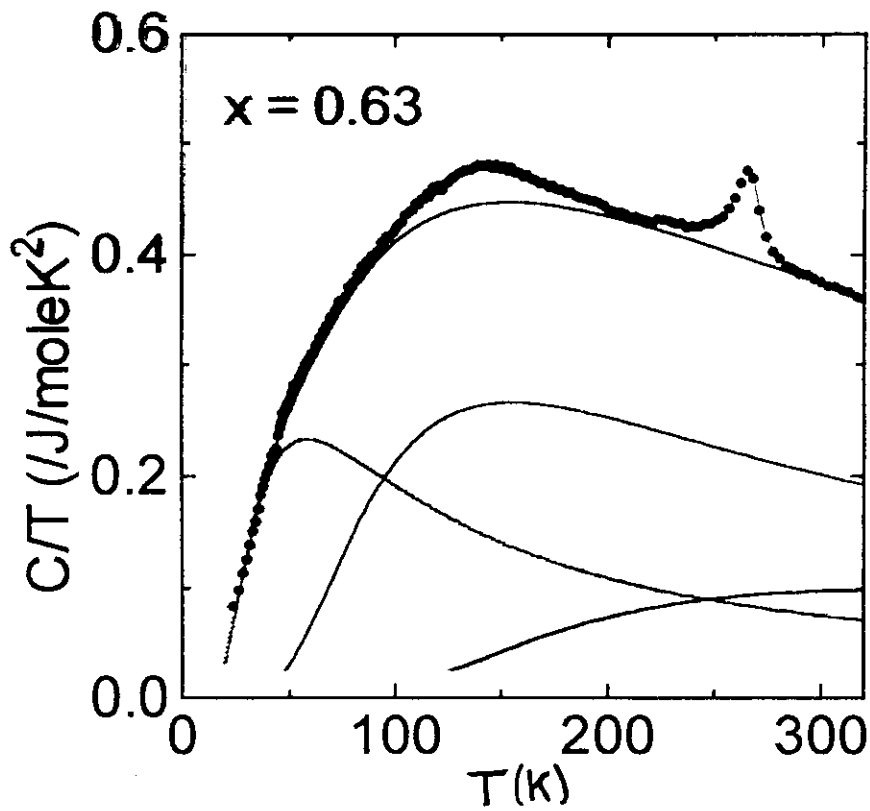


High-Temperature Specific heat - $La_{1-x}Ca_xMnO_3$

Main problem - large lattice background and no nonmagnetic isomorph. Fit the lattice with 3 optical level contributions, at $\Delta E_{opt.} = 150, 400, 850$ K.



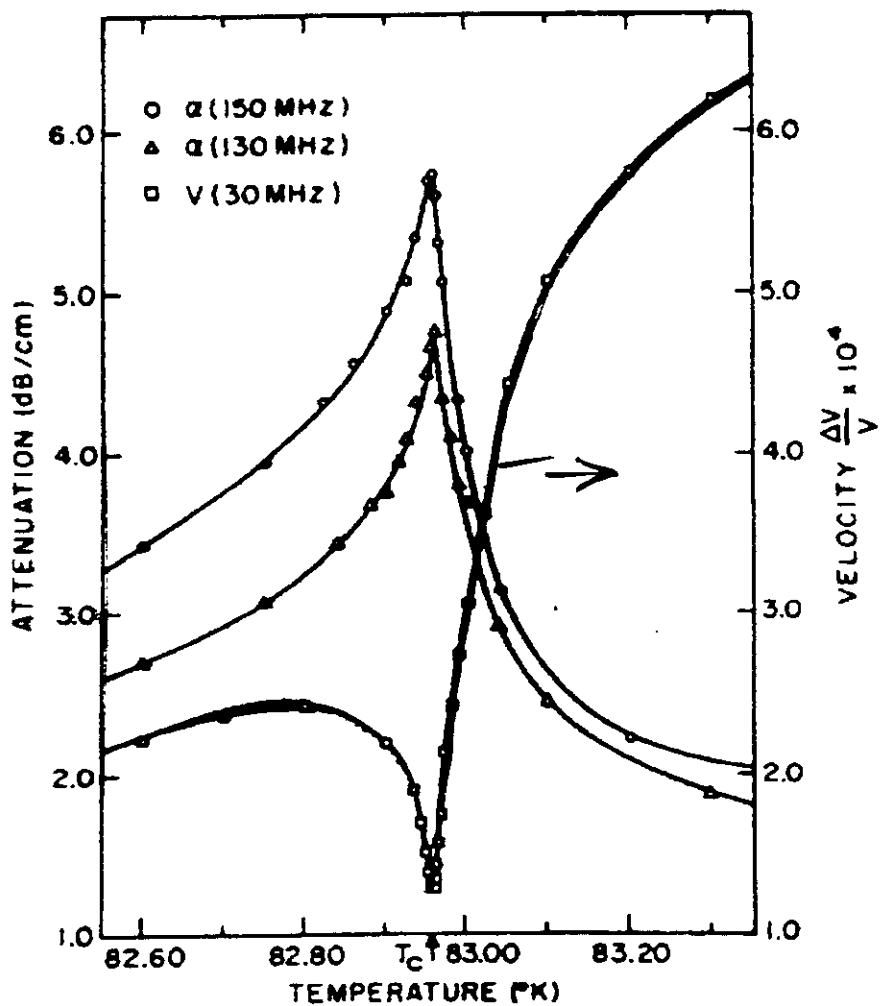
Ramirez et al. (1995)



What do we expect for sound velocity changes at an AF transition?

RbMnF₃

Golding (1968)



Sound Velocity in Ni
Alers et al., '60

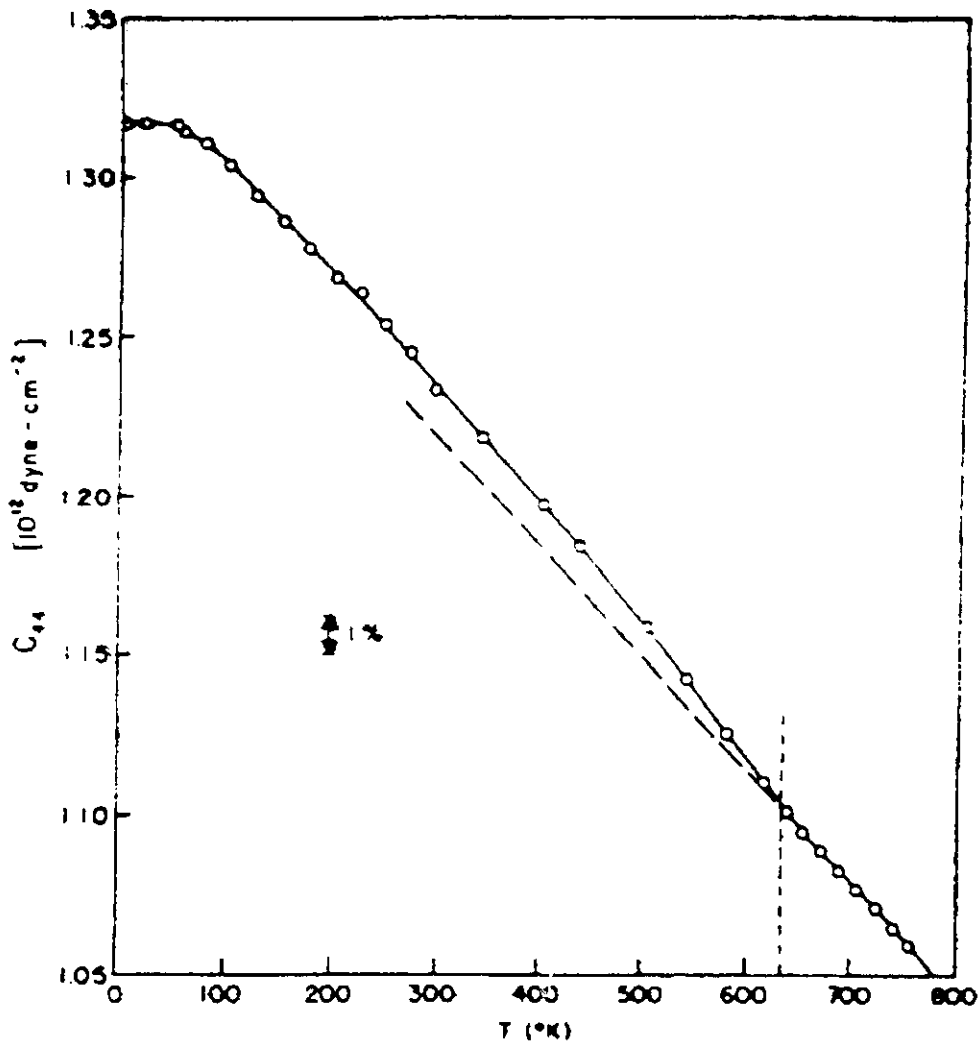
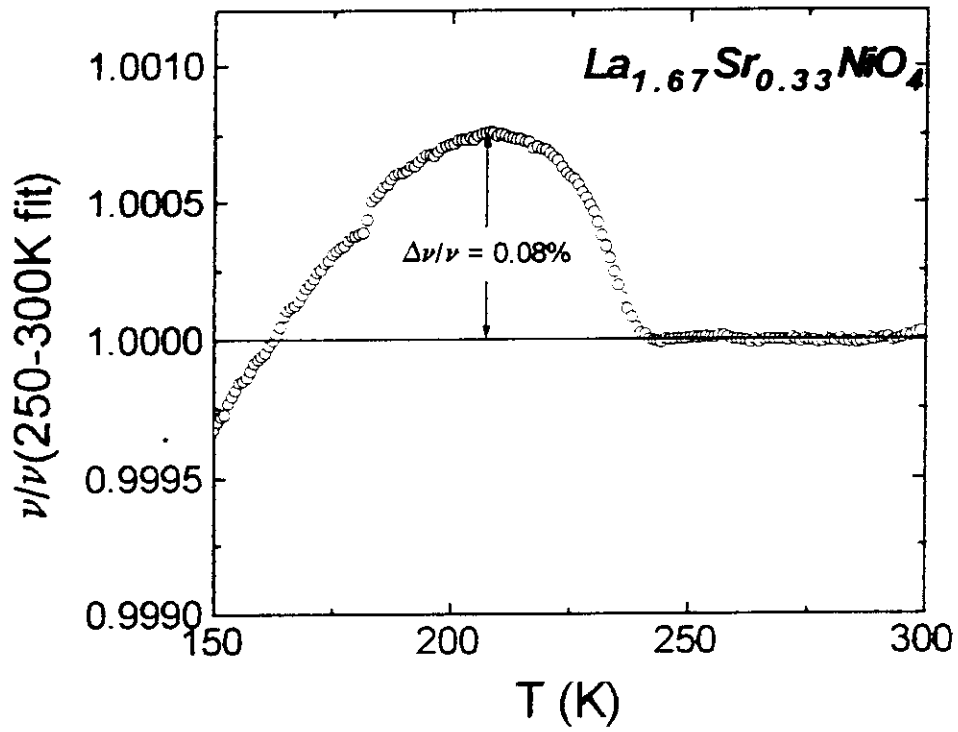


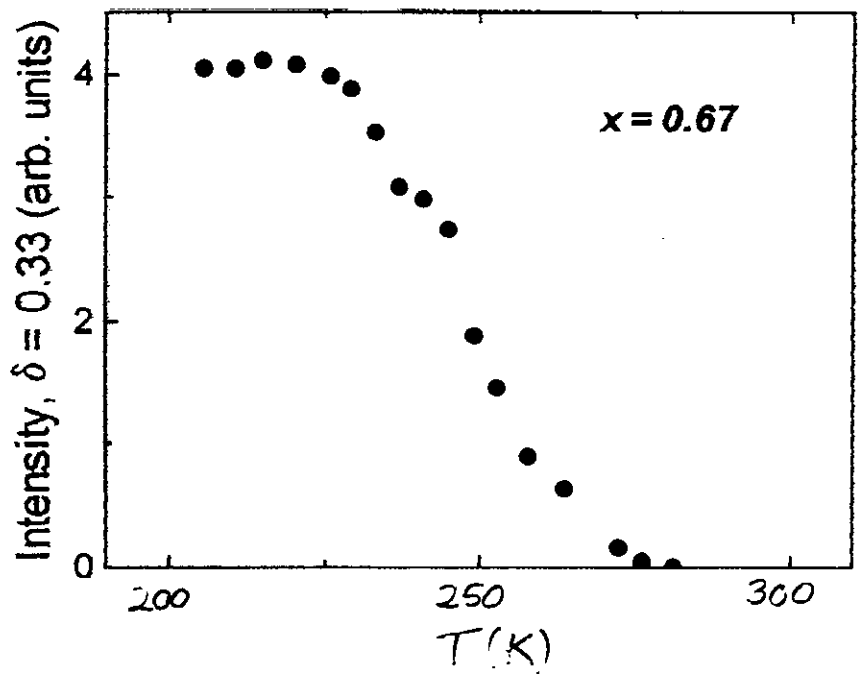
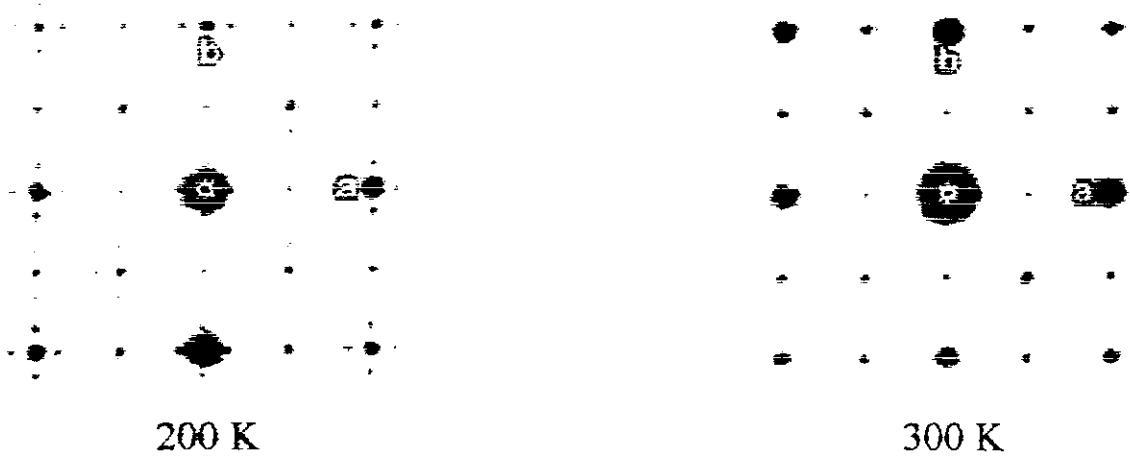
FIG. 1. Temperature variation of the elastic modulus C_{44} of nickel measured at 10 kOe applied field. The vertical dashed line marks the Curie temperature.

Compare the sound velocity change to the only other known charge-ordered system, $\text{La}_{1.67}\text{Sr}_{0.33}\text{NiO}_4$.



Transmission Electron-Diffraction evidence for Charge Ordering in $\text{La}_{0.33}\text{Ca}_{0.67}\text{MnO}_3$

Modulation wavevector $q = (2\pi/a)(\delta, 0, 0)$ with $\delta \approx 0.3$. Below, (a) and (b) are (200) and (020) respectively. (C. H. Chen)



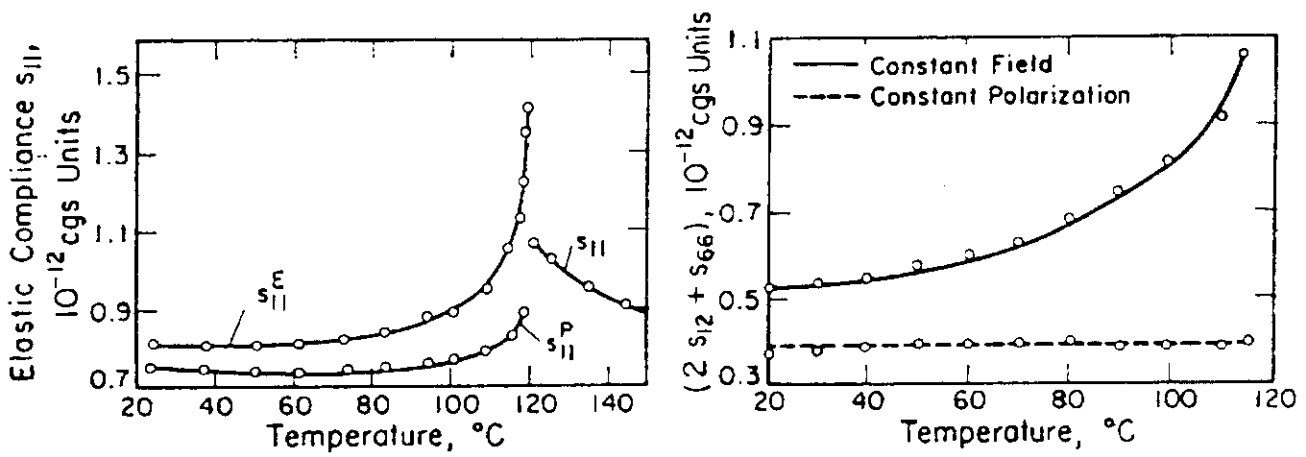
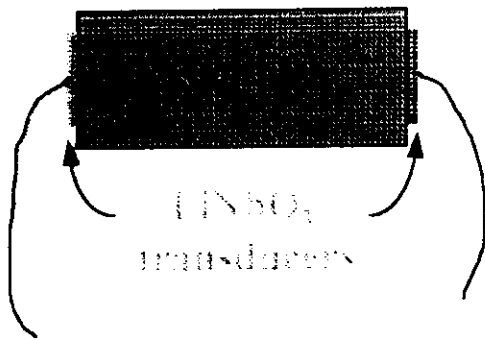


FIG. IV-31. Elastic behavior of BaTiO₃.

- (a) The compliance coefficients s_{11}^E and s_{11}^P as functions of temperature.
 (b) The quantities $(2s_{12} + s_{66})^E$ and $(2s_{12} + s_{66})^P$ as functions of temperature (according to Huibregtse *et al.* (H 3)).

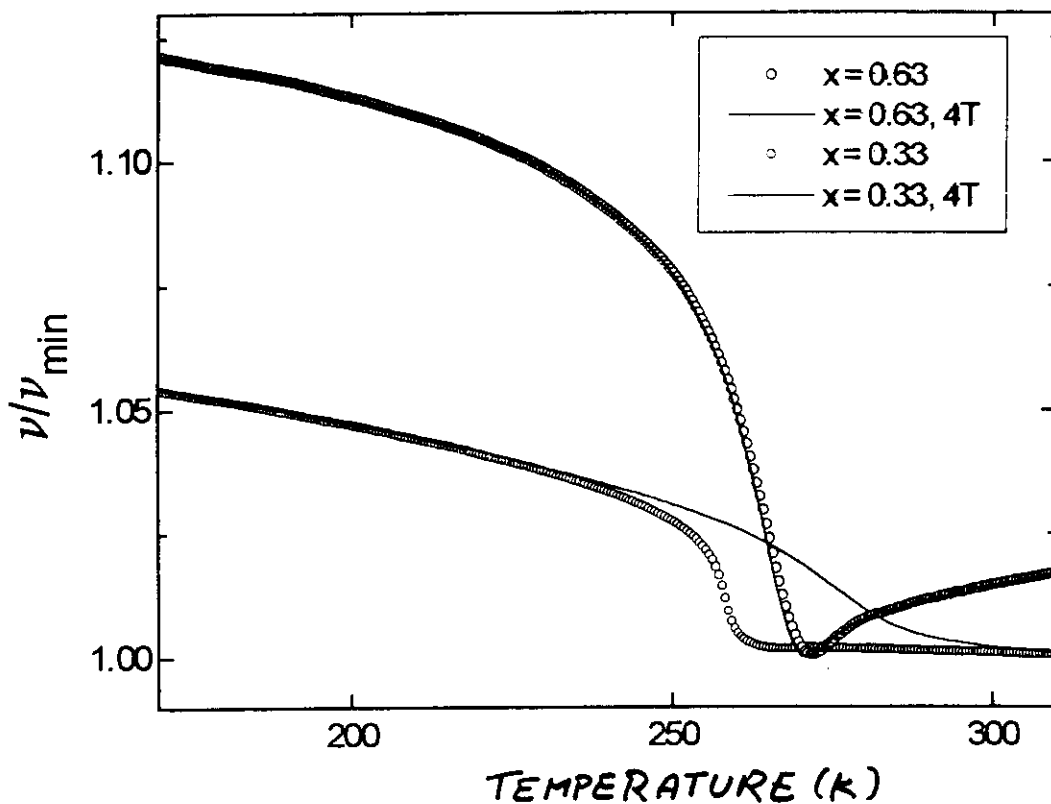
Sound Velocity in $\text{La}_{1-x}\text{Ca}_x\text{MnO}_3$:

Ramirez et al PRL, ~ April 96

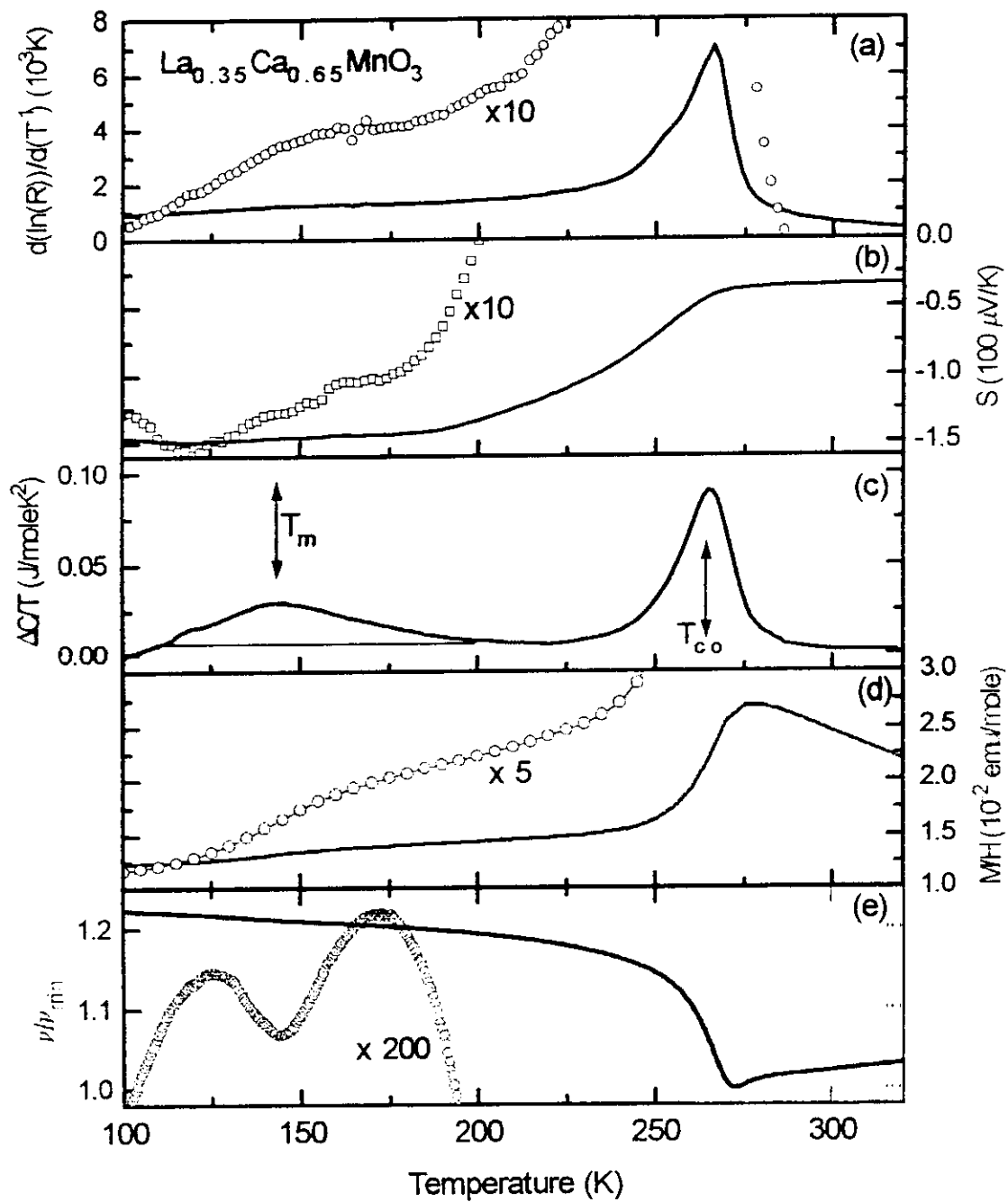


Sound velocity measured as frequency shift in a homodyne technique with digital feedback - typical frequencies are 10MHz

- FM phase ($x = 0.33$) large change due to direct coupling of sound to FM order parameter.
- CO phase ($x = 0.63$) large change due to strong electron-phonon coupling, $\times 100$ larger than in nickelate !



Evidence for separate CO and AF transitions in $\text{La}_{0.35}\text{Ca}_{0.65}\text{MnO}_3$



$\text{La}_{0.5}\text{Sr}_{1.5}\text{MnO}_4$ Peak Intensities

